lipopolysaccharide (LPS)-induced increase of proinflammatory cytokines, IL-1β and TNF-α, in BV-2 microglia cell line. In addition, MW01-5-188WH effectively suppressed human amyloid-β-induced glial activation and the increased production of proinflammatory cytokines in the hippocampus *in vivo*, with a resultant attenuation of synaptic dysfunction and improvement in hippocampus dependent behavioral deficits (Ralay Ranaivo et al., 2006). Previous studies have shown that other drugs with mechanisms of action that are different from MW01-5-188WH, such as indomethacin and minocycline, also inhibit microglial activation and restore or increase hippocampal neurogenesis (Ekdahl et al., 2003; Monje et al., 2003). However, to our knowledge, there was no report demonstrating an effect on EAE of a drug that inhibits glial activation. Considering the fact that activation of microglia and astrocyte is implicated in the pathogenesis of MS and EAE (Liedtke et al., 1998; Aharoni et al., 2005; Tanuma et al., 2006), it would be of great interest to know whether MW01-5-188WH or future refined analogs of this new class of compounds might be effective for MS. To determine this possibility, we examined the effect of MW01-5-188WH on myelin oligodendrocyte glycoprotein (MOG)-induced EAE mice. Our data showed that MW01-5-188WH ameliorated the severity of EAE by inhibiting the activation of glial cells.

2. Materials and methods

2.1. Mice

Female C57BL/6J mice were obtained from the CLEA Japan (Tokyo, Japan) and maintained at the animal facilities of the Tokyo Metropolitan Institute for Neuroscience. All mice were 6 weeks of age at the time of immunization. Animal treatments were performed in accordance with the Tokyo Metropolitan Institute for Neuroscience *Guidelines for the Care and Use of Animals.*

2.2. EAE induction, MW01-5-188WH administration and clinical scoring

EAE was induced by immunization with rat MOG_{35-55} peptide (MEVGWYRSPFSRVVHLYRNGK) synthesized by an automated peptide synthesizer (model PSSM-8; Shimazu, Kyoto, Japan). Mice were injected subcutaneously at one side of the flanks with 200 μg of rat MOG in complete Freund's adjuvant (Difco Laboratories, Detroit, MI) and 500 μg of *Mycobacterium tuberculosis* H37 RA (Difco). An identical booster was given at the other flank 1 week later. Mice also received intraperitoneal injections of 500 ng pertussis toxin (Seikagaku, Tokyo, Japan) in 200 μl PBS immediately after the first MOG injection and 48 h later. MOG-immunized mice were administrated by oral gavage either MW01-5-188WH (5 mg/kg, treated group) or diluent (10% DMSO, vehicle group) in a 5% acacia suspension once daily according to the following treatment schedules: 1, treatment solely in the induction phase (d0–d12); 2, treatment solely in the effector phase (d13–d30); 3, treatment throughout the whole period of the experiment (d0–d30).

Mice were scored daily for signs of EAE on a scale of 0–9 using the following criteria: 0, no clinical signs; 1, partial tail paralysis; 2, complete tail paralysis; 3, impairment of righting reflex; 4, partial hind limb paralysis; 5, complete hind limb paralysis; 6, partial body paralysis; 7, partial forelimb paralysis; 8, complete forelimb paralysis or moribund; 9, death.

2.3. Spinal cord pathology and immunohistochemistry

On day 30 after immunization, age-matched normal non-immunized mice (normal group), vehicle group and treated group mice were anesthetized with diethylether and perfused transcardially with saline, followed by 4% paraformaldehyde in 0.1 M phosphate buffer containing 0.5% picric acid. The lumbar spinal cords (L1–L3) were removed and postfixed in the same fixative for 2 h at 4 °C and immersed in 30% sucrose in 66 mM phosphate buffer (PB; pH 7.4). Then the spinal cords were embedded in optimal cutting temperature (OCT) compound (Tissue-Tek, Tokyo, Japan) and frozen on dry ice. Cryostat sections (10 μm) were cut coronally and collected on MAS-coated slides (Matsunami, Osaka, Japan). For pathological study, sections were stained with Luxol fast blue (LFB) followed by hematoxylin and eosin (H&E). Immunohistochemistry was performed as previously described (Harada et al., 2006). Briefly, the sections were blocked with phosphate-buffered saline (PBS; pH 7.4) containing 1% normal horse serum and 0.4% Triton-X 100 for 1 h at room temperature. They were incubated overnight at 4 °C with the following primary antibodies: rabbit anti-iba1 (1.0 μg/ml; Harada et al., 2002), rabbit anti-GSTπ (2.0 μg/ml; Medical and Biology Lab, Nagoya, Japan) and mouse anti-GFAP (50 μg/ml; Progen, Heidelberg, Germany), markers for microglia, oligodendrocytes and astrocytes, respectively. The sections were then incubated with Cy-2-conjugated donkey anti-mouse IgG (Jackson ImmunoResearch, West Grove, PA), Cy-2-conjugated donkey anti-rabbit IgG (Jackson ImmunoResearch) or DAKO EnVision (DAKO, Glostrup, Denmark) and DAB substrate kit (DAKO). In some experiments, nuclear staining was performed using Hoechst 33342 (10 μM; Invitrogen, Carlsbad, CA).

2.4. Microscopy and quantification

Stained sections were examined with a microscope (BX51; Olympus, Tokyo, Japan) equipped with Plan Fluor objectives connected to a DP70 camera (Olympus). To quantify immunostaining results, three sections from the spinal cord L1–L3 of each mouse were examined, with three mice per experimental group, for a total of nine sections per experimental group. Digital images from a same area (0.143 mm^2) of the middle region of the ventral horn were captured, and iba1+, GFAP+, GSTπ/Hoechst 33342 double-stained cells in each group were counted from the images. The counting results for each group were averaged and expressed as mean percentage changes compared with age-matched normal group.

2.5. Cell culture

Primary astrocyte and microglia cells were obtained as previously reported (Ohsawa et al., 2007). Cerebral cortices from 1- to 3-day-old C57BL/6 mice were excised, meninges removed and cortices minced into small pieces. Subsequently, the tissue was dissociated by incubation with 0.25% trypsin at 37 °C for 15 min, and the resultant tissue suspension was triturated to yield a single cell suspension. The cells was centrifuged for 5 min at 800 rpm and seeded on a 75 cm^2 tissue culture flask in Dulbecco's Modified Eagle Medium (DMEM) containing 10% fetal bovine serum (FBS). Complete confluence was reached in 7–10 days at 37 °C/5% CO_2. Flasks were then shaken 2 h (150 rpm at 37 °C) in a temperature-controlled shaker to loosen microglia and oligodendrocytes from the more adherent astrocytes. These less adherent cells were plated for 2 h and then lightly shaken to separate oligodendrocytes from the more adherent microglia. Microglia were seeded in 96-well plates (2.5×10^4 cells/well) and incubated 2 h at 37 °C/5% CO_2 before stimulation. After shaking to remove microglia and oligodendrocytes, astrocytes were recovered by trypsinization, seeded in 96-well plates (5×10^4 cells/well) and cultured for 2 days. The above microglia and astrocytes were treated in serum-free media for 16 h either with no stimulus or one of the following three stimuli: LPS (2500 ng/ml), IFN-γ (250 ng/ml) and TNF-α (250 ng/ml), in the presence of diluent or MW01-5-188WH (7.5 and 75 μM for microglia and astrocyte, respectively). Stock solutions (20 mM) of MW01-5-188WHWH are prepared in DMSO. Solutions for cell treatments were prepared by dilution of stock solutions into serum-free media immediately before adding to the cells. Finally, tissue culture supernatants were collected and processed for enzyme-linked immunosorbent assay (ELISA) assays. Control wells contained the same final concentration of DMSO as the compound-containing wells, and the cell viability after treatments was determined by Cell Counting Kit-8 (Dojindo, Kumamoto, Japan).

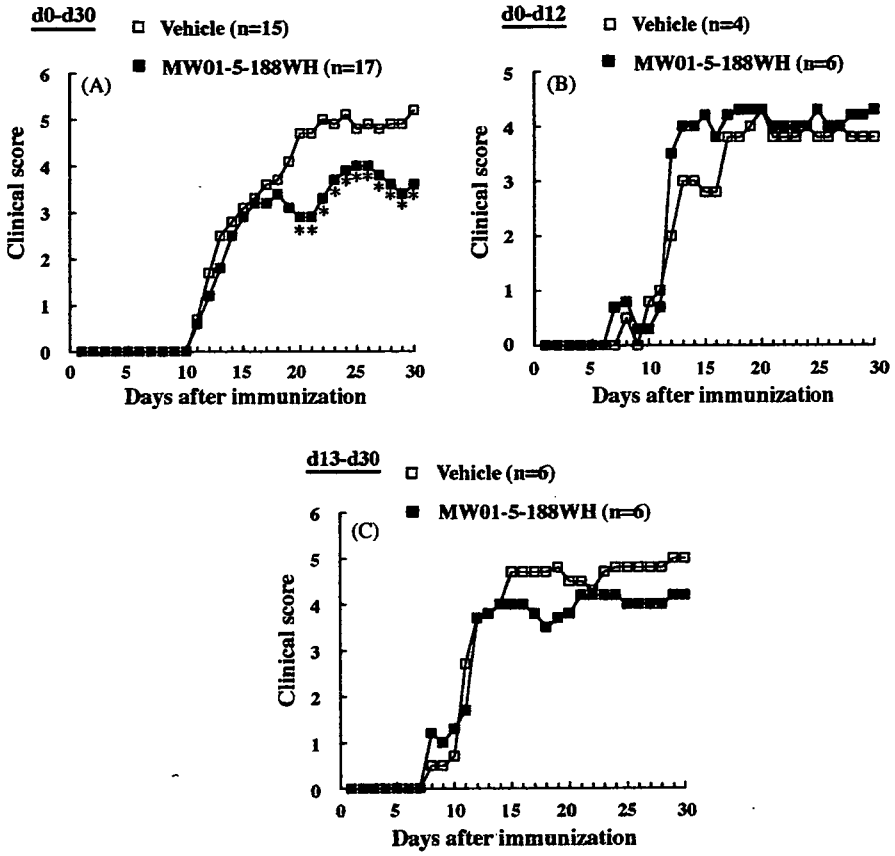

Fig. 1. Effect of MW01-5-188WH on the severity of MOG-induced EAE mice. Mice were orally administrated with MW01-5-188WH (5 mg/kg) or vehicle (10% DMSO in DW) in a 5% acacia suspension in three time frames: the whole experiment period (d0–d30; A), the induction phase (d0–d12; B) and the effector phase (d13–d30; C), and daily mean clinical courses of EAE in mice were shown. When mice were treated for the whole experiment period (A), significant difference in clinical scores between the treated group and vehicle group was found from d20 to d30. When mice were treated only in the induction period (B) or the effector period (C), although no significant differences were found for both two treatments, a tendency of lower scores was found in the effector phase treatment (C). d, days after immunization. $^{*}p < 0.05$.

2.6. Quantitative real-time PCR analysis of chemokines in vivo

A quantitative reverse transcription-polymerase chain reaction assay (qRT-PCR) was performed to measure the expression levels of three chemokine mRNA transcripts (MCP-1, RANTES and IP-10) in the spinal cord as previously reported (Namekata et al., 2006). Total RNA of lumbar spinal cords (L1–L3) freshly dissected from normal, vehicle and MW01-5-188WH-treated EAE mice, which were sacrificed on day 30 after immunization, was extracted with Isogen (Nippon Gene, Tokyo, Japan) according to manufacture's protocol. Resultant RNA was treated with DNase (RQ1 RNase-free DNase, Promega, Madison, WI) and reverse-transcribed with Revertra ace (Toyobo, Osaka, Japan) to obtain cDNA. Quantitative RT-PCR was performed with the ABI 7500 fast real-time PCR system (Applied Biosystems, Foster City, CA) with SYBR Green PCR Master Mix (Applied Biosystems) according to manufacturer's protocol. Thermocycling of each reaction was performed with each primer at a concentration of 100 nM (RANTES: forward primer 5′-GCC CAC GTC AAG GAG TAT TT-3′, reverse primer 5′-TGA CAA ACA CGA CTG CAA GA-3′; IP-10: forward primer 5′-GCT GCA ACT GCA TCC ATA TC-3′, reverse primer 5′-TTT CAT CGT GGC AAT GAT CT-3′; MCP-1: forward primer 5′-AAC TGC ATC TGC CCT AAG GT-3′, reverse primer 5′-ACG GGT CAA CTT CAC ATT CA-3′). The following protocol was used: denaturation program (95 °C for 3 min), followed by the amplification and quantification program (95 °C for 15 s and 60 °C for 30 s) repeated for 50 cycles. The PCR quality and specificity were verified by melting curve analysis. A standard curve of cycle thresholds using serial dilutions of cDNA samples were used to calculate the relative abundance. The difference in the initial amount of total RNA between the samples was normalized in every assay using a glyceraldehyde-3-phosphate

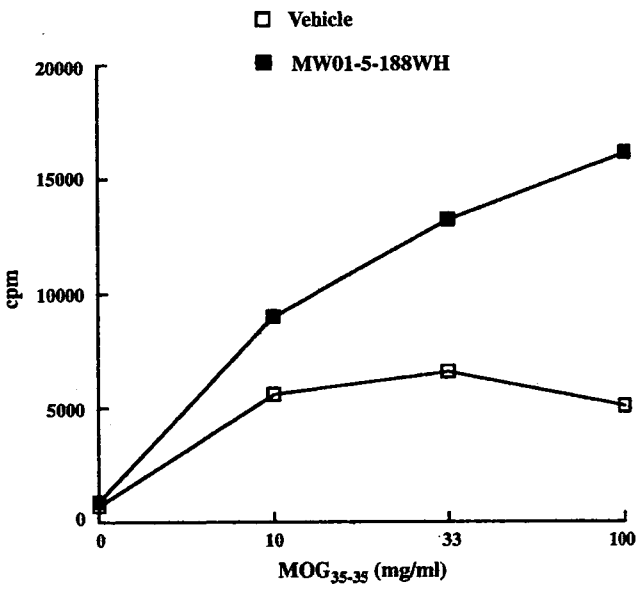

Fig. 2. Effect of MW01-5-188WH on proliferative responses of MOG-specific T cells. Proliferative responses of lymph node cells (3×10^5 cells/well) to MOG at the indicated concentrations were measured 12 days after MOG immunization. No significant difference was found between the two groups.

dehydrogenase (G3PDH) gene expression as an internal standard (forward primer 5′-TGC ACC ACC AAC TGC TTA G-3′, reverse primer 5′-GGA TGC AGG GAT GAT GTT C-3′).

2.7. ELISA

Chemokine (RANTES, MCP-1, IP-10) levels in cell culture media were determined by ELISA according to the manufacturer's instructions (BioSource, Camarillo, CA; R&D Systems, Minneapolis, MN). Optical densities were measured using a Model 550 microplate reader (Bio-Rad, Hercules, CA) at 450 nm. Chemokine concentrations in media were calculated from standards containing known concentrations of the proteins.

2.8. Proliferation assay

Proliferative responses of lymph node (LN) cells from vehicle and MW01-5-188WH-treated mice were assayed in microtiter wells by uptake of [^{3}H]thymidine in accord with the procedure reported elsewhere (Arimoto et al., 2000). After washing with PBS, LN cells (3×10^5 cells/well) were cultured with given concentrations of MOG_{35-55} for 3 days, with the last 18 h in the presence of

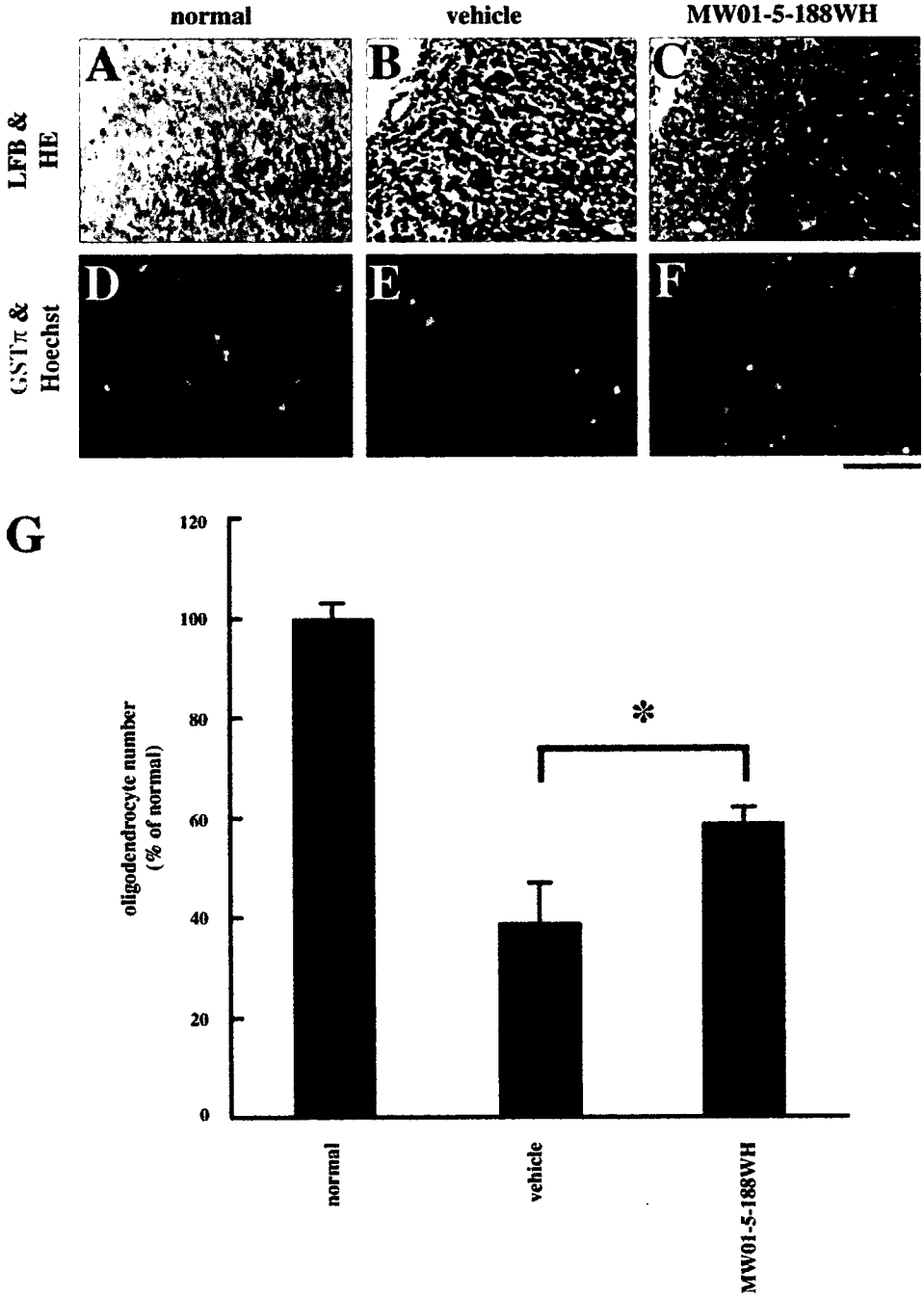

Fig. 3. Effect of MW01-5-188WH on the extent of demyelination and oligodendrocyte cell death in EAE mice. (A–C) Representative LFB- and H&E-stained region of lateral funiculus of spinal cords from non-EAE normal (A), vehicle (B)- and MW01-5-188WH (C)-treated EAE mice. (D–F) GSTπ and Hoechst33342 double-stained region of gray matter of spinal cords from non-EAE normal (D), vehicle (E)- and MW01-5-188WH (F)-treated EAE mice. (G) Quantification of oligodendrocytes presented as percentage of normal. Results of three independent animals are presented as mean ± S.E.M. Note the increased oligodendrocyte number after MW01-5-188WH treatment. Scale bar: 100 μm in (A–C) and 70 μm in (D–F). $^*p < 0.05$.

0.5 μCi [^{3}H]thymidine (GE Healthcare Bioscience, Tokyo, Japan). The cells were harvested on glass-fiber filters, and the label uptake was determined using standard liquid scintillation techniques.

2.9. Statistics

Data are presented as mean ± S.E.M. except otherwise noted. Student's *t*-test was used to estimate the significance of difference in results. Statistical significance was accepted at $p < 0.05$.

3. Results

3.1. Effect of MW01-5-188WH on clinical course of EAE

We examined the effect of MW01-5-188WH by daily oral administration from 0 to 30 days after the disease induction (d0–d30). Clinical signs of EAE in vehicle and MW01-5-188WH-treated groups developed 13.5 ± 0.8 ($n = 15$) and 12.6 ± 0.4 ($n = 17$) days after the first MOG immunization, and no significant difference was found between the groups ($p = 0.168$, Fig. 1A). On the other hand, the daily mean clinical scores were lower in the MW01-5-188WH-treated group compared to the vehicle group, but significant differences were first detected at d20 ($p = 0.009$). The mean clinical scores of the vehicle and treated groups on d30 were 5.2 ± 0.4 and 3.6 ± 0.5, respectively ($p = 0.012$).

The initial immunopathological event of EAE starts when auto-reactive T cells in the systemic immune compartment are activated through the recognition of their specific antigen (induction phase), which finally leads to a stimulation of microglia/astrocytes in the central nervous system (effector phase) (Magnus and Rao, 2005). So, we next examined the effect of MW01-5-188WH on the antigen-specific T cell proliferation and representative data from one mouse of each group was shown in Fig. 2. Freshly isolated T cells from the drug- and vehicle-treated mice both responded to MOG at any of the concentrations tested, but no significant difference was found between the two groups. This result indicates that MW01-5-188WH does not modulate the immune response in EAE mice at a dose that alters clinical presentation.

We also examined the effect of MW01-5-188WH in two different time frames, namely in the induction phase (d0–d12) and in the effector phase (d13–d30). When EAE mice were treated solely in the induction phase, no significant difference of clinical scores was found in vehicle and MW01-5-188WH-treated groups (Fig. 1B). When mice were treated in the effector period, although no significant differences was detected, a tendency of lower scores was found in the MW01-5-188WH-treated group (Fig. 1C). These results suggest that MW01-5-188WH ameliorates the severity of MOG-induced EAE by mainly inhibiting the glial activation in the effector phase.

3.2. Effect of MW01-5-188WH on pathology of EAE

We next examined the histological basis of MW01-5-188WH's protective effect on the EAE clinical score. LFB and H&E staining showed that MOG immunization induced inflammation and demyelination in the mouse spinal cord (Fig. 3A–C). Numerous inflammatory cell infiltrates were observed in the white matter of the spinal cord in the vehicle group (purple dots in Fig. 3B) relative to that in the normal group (Fig. 3A). And areas containing myelin were decreased in the vehicle group compared with that in the normal group (blue areas in Fig. 3A and B). MW01-5-188WH treatment significantly reduced inflammation and demyelination (Fig. 3C). In addition, this improvement was accompanied by an increased survival rate of oligodendrocytes in the treated group (Fig. 3F) compared with the vehicle group (Fig. 3E). Quantitative analysis revealed that the percentage of surviving GSTπ-positive oligodendrocytes increased from 39 ± 7% in the vehicle group to 60 ± 3% in the treated group ($p < 0.05$, Fig. 3G). These results suggest that MW01-5-188WH improved pathology of MOG-induced EAE by suppressing

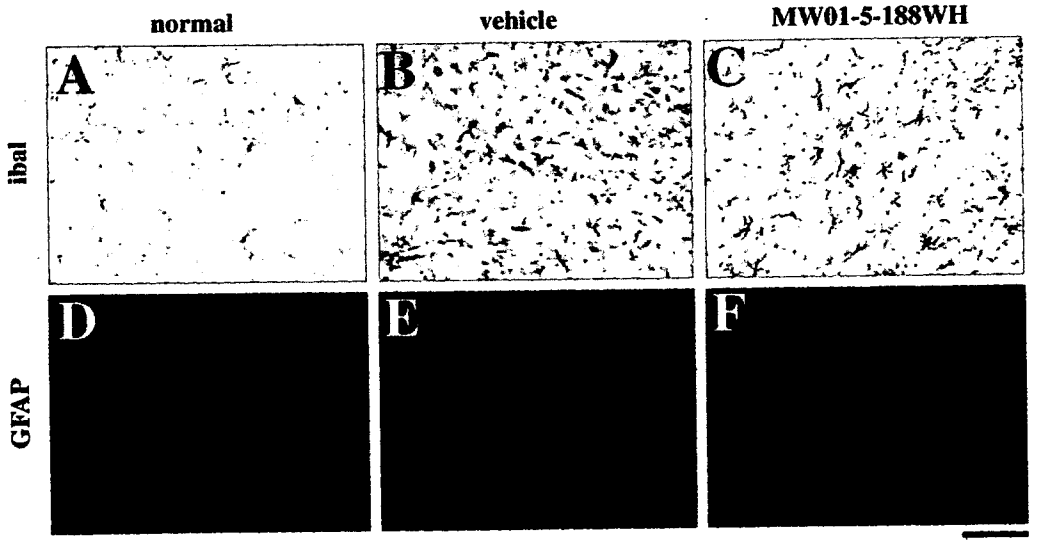

Fig. 4. Effect of MW01-5-188WH on glial activation in EAE mice. Representative iba1 (A–C)- and GFAP (D–F)-stained region of gray matter of spinal cords from non-EAE normal (A and D), vehicle (B and E)- and MW01-5-188WH (C and F)-treated EAE mice. Scale bar: 50 μm.

inflammation, demyelination and depletion of oligodendrocytes.

3.3. Effect of MW01-5-188WH on the activity of microglia and astrocytes in EAE

Microglia and astrocytes in the spinal cord are activated upon EAE induction (Liedtke et al., 1998; Aharoni et al., 2005). We determined these phenomena in our EAE model, and found that the number of iba1-positive microglia was increased (Fig. 4B) compared with the normal group (Fig. 4A). Since MW01-5-188WH selectively inhibits the activation of glial cells (Ralay Ranaivo et al., 2006), we next examined its effect on microglial activation in our EAE model. Daily oral administration of MW01-5-188WH decreased the number of microglia from 650 ± 7% in the vehicle group to 340 ± 13% ($p = 0.003$, Fig. 5A). Activated form of microglia was also decreased by this treatment (Fig. 4C). Similarly, the number of GFAP-positive astrocytes was increased upon EAE induction (Fig. 4E) compared with that in the normal group (Fig. 4D). MW01-5-188WH treatment also suppressed the increase from 242 ± 7% in the vehicle group to 158 ± 2% in the treated group ($p = 0.002$, Figs. 4F and 5B). Taken together, these results suggest that MW01-5-188WH treatment had inhibitory effects on the activity of microglia and astrocytes in EAE.

3.4. Effect of MW01-5-188WH on chemokine production in vivo and in vitro

Activated microglia and astrocytes produce various chemokines such as RANTES, IP-10 and MCP-1 that have been shown to contribute to the disease progression of MS and EAE (Balashov et al., 1999; Juedes et al., 2000). To determine whether MW01-5-188WH suppresses the *in vivo* increase in the concentration of these three chemokines, we first investigated the chemokine production levels in the spinal cord. When EAE was induced, all three chemokines' mRNA transcripts in the spinal cord were increased as shown in Fig. 6. While there was a tendency of lower expression levels of three chemokines in MW01-5-188WH-treated mice, no significant difference was found compared with the vehicle group. Since this method may mask the effect of MW01-5-188WH on chemokine productions in glial cells, we next examined its effect directly on cultured microglia and astrocytes. We prepared primary cultured microglia and astocytes, and stimulated them with LPS, IFN-γ or TNF-α in the presence or absence of compound. Release of RANTES was increased by all three stimuli and MW01-5-188WH significantly suppressed its release from both microglia (Fig. 7A) and astrocytes (Fig. 8A). MW01-5-188WH also suppressed the release of IP-10 from astrocytes (Fig. 8B), but it was effective only when stimulated by TNF-α in microglia (Fig. 7B). Similar variance was observed for MCP-1. MW01-5-188WH suppressed its release when stimulated by LPS or IFN-γ in microglia (Fig. 7C), whereas it was effective for LPS and TNF-α in astrocytes (Fig. 8C). MW01-5-188WH and all three stimuli did not kill microglia and astrocytes (data not shown), indicating that the suppression of chemokine release by MW01-5-188WH was not due to its effect on cell viability. These results suggest that MW01-5-188WH, at least partially, suppresses the number and activity of microglia and astrocytes, which may lead to the improvement of clinical signs and pathology in EAE.

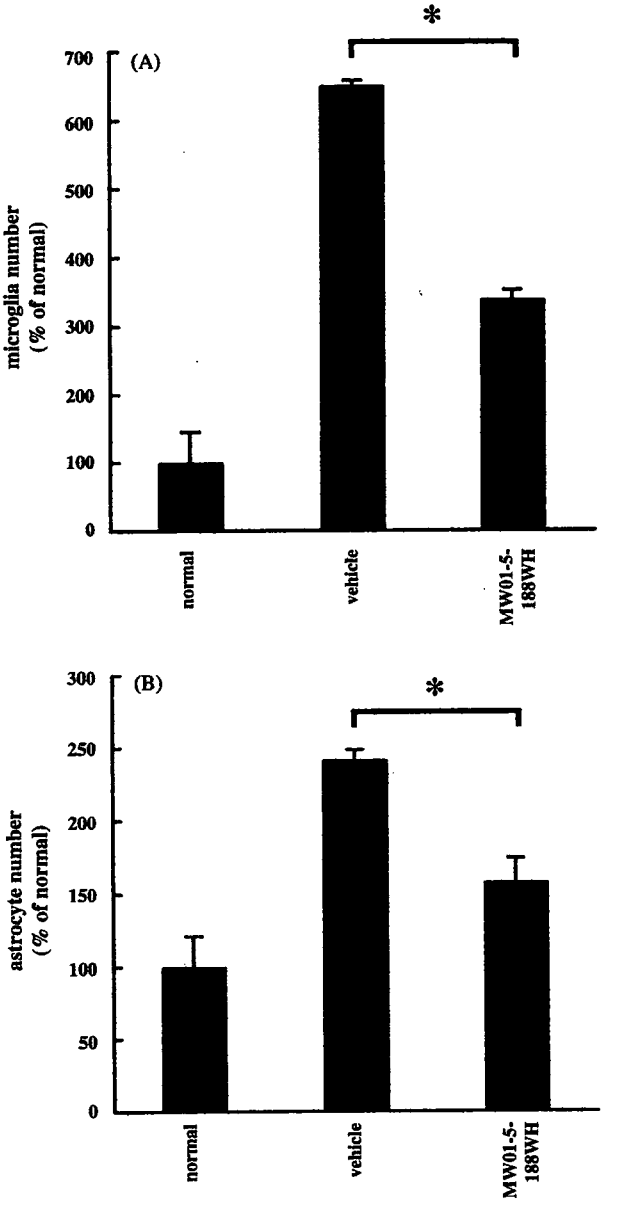

Fig. 5. Effect of MW01-5-188WH on glial cell number in EAE mice. Quantitative analysis of cell number in microglia (A) and astrocytes (B) in EAE mice presented as percentage of normal. Results of three independent experiments are presented as mean ± S.E.M. Note the decreased number in microglia and astrocytes after MW01-5-188WH treatment. $^{*}p < 0.05$.

4. Discussion

The initial immunopathological event of EAE and MS starts when auto-reactive T cells in the systemic immune compartment are activated and cross the blood–brain barrier and re-encounter their antigen (Magnus and Rao, 2005). This

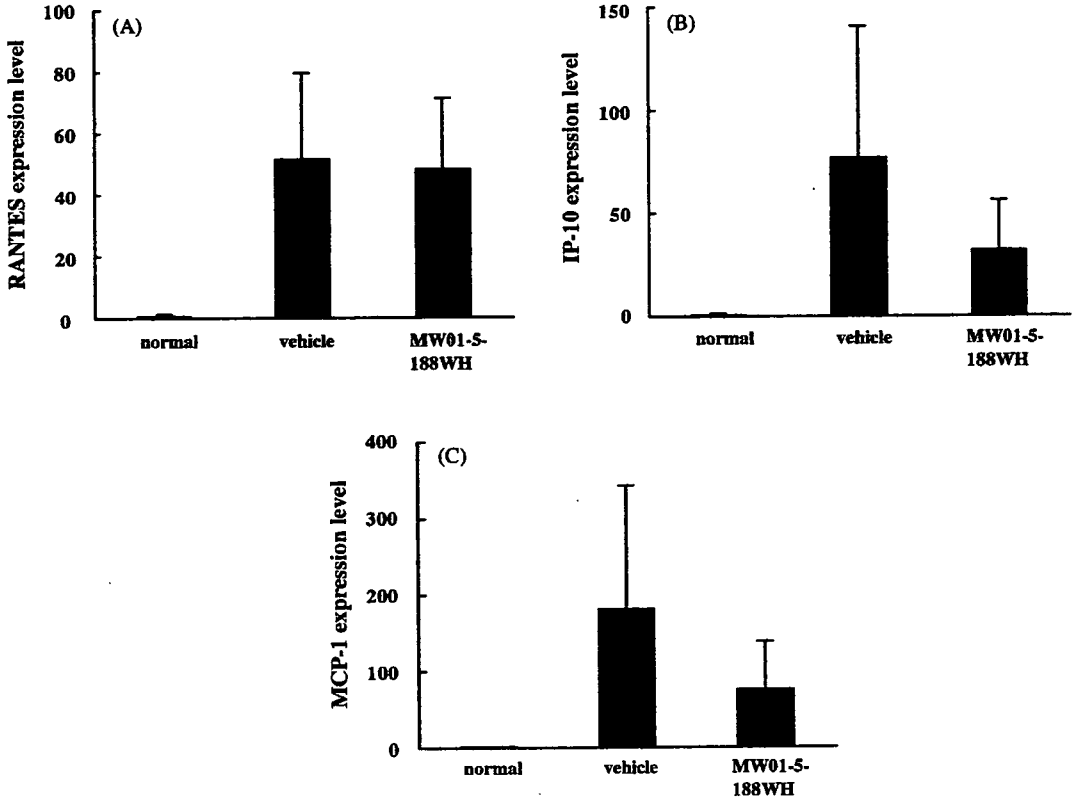

Fig. 6. Effect of MW01-5-188WH on chemokine production *in vivo*. mRNA expression levels of RANTES (A), IP-10 (B) and MCP-1 (C) in the spinal cords dissected from different treatment groups were measured by quantitative RT-PCR. Data in vehicle- and MW01-5-188WH-treated groups were normalized according to those in the normal group.

encounter leads to a reactivation and expansion of the autoreactive T cells that in turn stimulates microglia/astrocytes to increase their activities, to release more proinflammatory cytokines and chemokines. The release of these mediators induces demyelination and axonal degeneration. Based on the fact that MS and EAE are inflammatory diseases associated with activated glial cells, interventions targeting the immune response or the reactive glia seem to be possible. Over the last decades, changing the direct immune response has been the main strategy of multiple studies (Matsumoto and Fujiwara, 1993; Aharoni et al., 2005). And the current treatment of MS is based on immune modulators such as glatiramer acetate (Neuhaus et al., 2000; Kieseier and Hartung, 2003) or immune suppressors such as mitoxantrone (Hartung et al., 2002). However, almost no pharmacological study has been done on the treatment of EAE with reactive glial cells as the main targets. In the present study, we focused on a therapeutic strategy on targeting reactive glia using a novel CNS drug that has never been applied for EAE. We tested whether the administration of MW01-5-188WH is effective for the treatment of EAE.

MW01-5-188WH is a novel CNS drug designed to target glial activation (Ralay Ranaivo et al., 2006). Our *in vivo* results showed that the oral administration of MW01-5-188WH reduced both the clinical and pathological severities of EAE. MW01-5-188WH has been demonstrated *in vivo* to effectively suppress human amyloid-β-induced glial activation and decrease the production of proinflammatory cytokines in the hippocampus. In our present study, consistent with previous studies (Liedtke et al., 1998; Aharoni et al., 2005), activation of microglia and astrocytes was observed in the spinal cord of EAE mice. MW01-5-188WH administration at 5 mg/kg inhibited this glial activation, and resulted in the improvement of clinical scores and a partial rescue of oligodendrocytes from cell death. On the other hand, MW01-5-188WH administration at this low dose did not alter the proliferation response of T cells from mice immunized with MOG. Furthermore, the drug administered during the induction phase had no effect on the severity of EAE. Thus, this drug does not seem to have major effect on the immune system at an effective dose that brings about attenuation of glial activation. Certainly, no significant differences were found when MW01-5-188WH was administrated in the effector phase (d13–d30) solely, but glial activation might have been partially induced in the "initiation phase", especially during d10–d12, in animals demonstrating EAE signs before d13 (Fig. 1C). Another concern is that selectivity of pharmacological effects on activation of T cells or B-cells over a range of doses remains to be determined for the drug candidate compound MW01-5-188WH. Craft et al. (2006) previously showed in early integrative chemical biology studies that the bioavailable compound MW01-070C could suppresses CNS inflammatory responses at doses that did not suppress peripheral immune responses including T cell and B cell activation. Taken in their entirety, the available

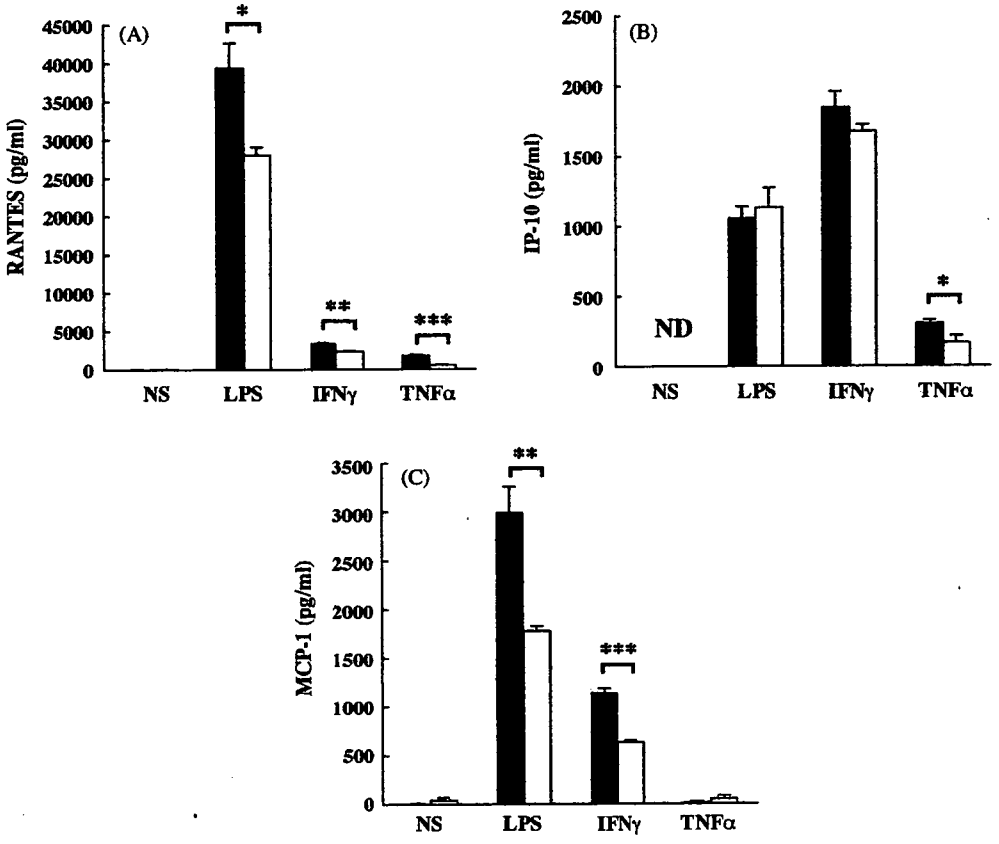

Fig. 7. Effect of MW01-5-188WH on chemokine production by microglia. Cells were treated for 16 h with or without 7.5 μM MW01-5-188WH under non-stimulation, or stimulation with LPS (2500 ng/ml), IFN-γ (250 ng/ml) or TNF-α (250 ng/ml). RANTES (A), IP-10 (B) and MCP-1 (C) levels were determined in culture medium by ELISA. Values represent the mean ± S.E.M. for a representative experiment run in quadruplicate. Note the decreased chemokine production by microglia after MW01-5-188WH treatment. NS, no stimulus; ND, non-detectable. $^{*}p < 0.05$, $^{**}p < 0.01$, $^{***}p < 0.001$.

data provide a proof-of-concept that it is possible to selectively restore excessive proinflammatory responses in the CNS back towards homeostasis at doses of a peripherally administered compound that do not suppress systemic immune and inflammatory responses. Thus, our results support the concept that glial cells are possible therapeutic targets for MS (Heppner et al., 2005; Tanuma et al., 2006) as well as other neurodegenerative disorders (Harada et al., 2000, 2002; Farina et al., 2007).

Oligodendrocyte cell death occurs in the course of EAE. The factors mediating the death of oligodendrocytes can be summarized into two categories. One is the endogenous factors such as processed caspase-11 and activated caspase-3, leading to cell death via specific pathways (Hisahara et al., 2001). The other is the cytotoxic cytokines that are released from activated microglia and astrocytes, which may activate caspase cascades through their receptors in oligodendrocytes (Selmaj et al., 1991; Louis et al., 1993; Vartanian et al., 1995; Hisahara et al., 1997, 2001). MW01-5-188WH has been shown to suppress the release of proinflammatory cytokines such as IL-1β and TNF-α from microglia (Ralay Ranaivo et al., 2006). In addition, this drug significantly inhibited the release of RANTES, IP-10 and MCP-1 from primary cultured microglia and astrocytes. It is well known that chemokines are essential for inflammatory responses because they recruit specific subsets of leukocytes and monocytes into tissues (Luster, 1998; Zlotnik and Yoshie, 2000). For example, IP-10 is a strong candidate for recruiting T cell response and activated T cells express IP-10 receptor (Dufour et al., 2002; Christensen et al., 2004). $CD4^+$ and $CD8^+$ T cells and monocytes express RANTES receptor (Sorensen et al., 1999) and MCP-1 acts toward monocytes and T cells via type 2 CC chemokine receptor (CCR2; Sorensen et al., 1999). Therefore, MW01-5-188WH seems to reduce oligodendrocyte cell death, at least partly through the attenuation of microglia and astrocyte activation, which may subsequently reduce the release of key chemokines, infiltration of inflammatory cells, and spinal cord damage in EAE mice. Although further studies are needed, interfering with the interactions between glial cells might be a potential therapeutic strategy for the treatment of MS/EAE.

Acknowledgements

We thank Drs. K. Ohsawa, Y. Nakamura, and S. Kohsaka for their advice on microglia cell culture. This work was supported by grants from the Ministry of Education, Culture, Sports, Science and Technology of Japan (CH and TH), Naito Foundation and Uehara Memorial Foundation (TH). CH was supported by the Japan Society for the Promotion of Science for Young Scientists.

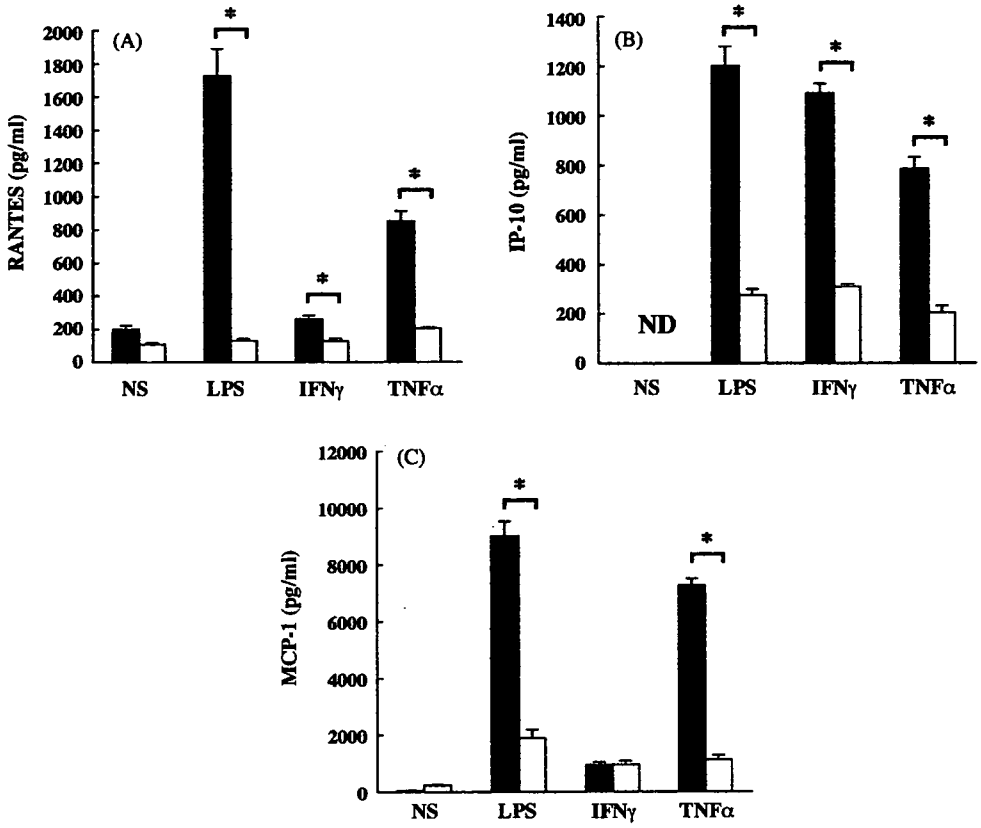

Fig. 8. Effect of MW01-5-188WH on chemokine production by astrocytes. Cells were treated for 16 h with or without 75 μM MW01-5-188WH under non-stimulation, or stimulation with LPS (2500 ng/ml), IFN-γ (250 ng/ml) or TNF-α (250 ng/ml). RANTES (A), IP-10 (B) and MCP-1 (C) levels were determined in culture medium by ELISA. Values represent the mean ± S.E.M. for a representative experiment run in quadruplicate. Note the decreased chemokine production by astrocytes after MW01-5-188WH treatment. NS, no stimulus; ND, non-detectable. $^{*}p < 0.001$.

References

Aharoni, R., Arnon, R., Eilam, R., 2005. Neurogenesis and neuroprotection induced by peripheral immunomodulatory treatment of experimental autoimmune encephalomyelitits. J. Neurosci. 25, 8217–8228.

Arimoto, H., Tanuma, N., Jee, Y., Miyazawa, T., Shima, K., Matsumoto, Y., 2000. Analysis of experimental autoimmune encephalomyelisis induced in F344 rats by pertussis toxin administration. J. Neuroimmunol. 104, 15–21.

Balashov, K., Rottman, J., Weiner, H., Hancock, W., 1999. CCR5+ and CXCR3+ T cells are increased in multiple sclerosis and their lignads MIP-1 and IP-10 are expressed in demyelinating braining lesions. Proc. Natl. Acad. Sci. U.S.A. 96, 6873–6878.

Christensen, J.E., Nansen, A., Moos, T., Lu, B., Gerard, C., Christensen, J.P., Thomsen, A.R., 2004. Efficient T-cell surveillance of the CNS requires expression of the CXC chemokine receptor 3. J. Neurosci. 24, 4849–4858.

Craft, J.M., Watterson, D.M., Van Eldik, L.J., 2006. Human amyloid β-induced neuroinflammation is an early event in neurodegeneration. Glia 53, 484–490.

Dufour, J.H., Dziejman, M., Liu, M.T., Leung, J.H., Lane, T.E., Luster, A.D., 2002. IFN-γ-inducible protein 10 (IP-10; CXCL10)-deficient mice reveal a role for IP-10 in effector T cell generation and trafficking. J. Immunol. 168, 3195–3204.

Ekdahl, C.T., Claasen, J.H., Bonde, S., Kokaia, Z., Lindvall, O., 2003. Inflammation is detrimental for neurogenesis in adult brain. Proc. Natl. Acad. Sci. U.S.A. 100, 13632–13637.

Farina, C., Aloisi, F., Meinl, E., 2007. Astrocytes are active players in cerebral innate immunity. Trends Immunol. 28, 138–145.

Glabinski, A.R., Tani, M., Strieter, R.M., Tuohy, V.K., Ransohoff, R.M., 1997. Synchronous synthesis of alpha- and beta-chemokines by cells of diverse lineage in the central nervous system of mice with relapses of chronic experimental autoimmune encephalomyelitis. Am. J. Pathol. 150, 617–630.

Godiska, R., Chantry, D., Dietsch, G.N., Gray, P.W., 1995. Chemokine expression in murine experimental allergic encephalomyelitis. J. Neuroimmunol. 58, 167–176.

Harada, C., Nakamura, K., Namekata, K., Okumura, A., Mitamura, Y., Iizuka, Y., Kashiwagi, K., Yoshida, K., Ohno, S., Matsuzawa, A., Tanaka, K., Ichijo, H., Harada, T., 2006. Role of apoptosis signal-regulating kinase 1 in stress-induced neural cell apoptosis *in vivo*. Am. J. Pathol. 168, 261–269.

Harada, T., Harada, C., Kohsaka, S., Wada, E., Yoshida, K., Ohno, S., Mamada, H., Tanaka, K., Parada, L.F., Wada, K., 2002. Microglia–Muller glia cell interactions control neurotrophic factor production during light-induced retinal degeneration. J. Neurosci. 22, 9228–9236.

Harada, T., Harada, C., Nakayama, N., Okuyama, S., Yoshida, K., Kohsaka, S., Matsuda, H., Wada, K., 2000. Modification of glial–neuronal cell interactions prevents photoreceptor apoptosis during light-induced retinal degeneration. Neuron 26, 533–541.

Hartung, H.P., Gonsette, R., Konig, N., Kwiecinski, H., Guseo, A., Morrissey, S.P., Karpf, H., Zwingers, T., 2002. Mitoxantrone in progressive multiple sclerosis: a placebo-controlled, double-blind, randomized, multicentre trial. Lancet 360, 2018–2025.

Heppner, F.L., Greter, M., Marino, D., Falsig, J., Raivich, G., Hovelmeyer, N., Waisman, A., Rulicke, T., Prinze, M., Priller, J., Becher, B., Aguzzi, A., 2005. Experimental autoimmune encephalomyelitis repressed by microglial paralysis. Nat. Med. 11, 146–152.

Hisahara, S., Shoji, S., Okano, H., Miura, M., 1997. ICE/CED-3 family executes oligodendrocyte apoptosis by tumor necrosis factor. J. Neurochem. 69, 10–20.

Hisahara, S., Yuan, J., Momoi, T., Okano, H., Miura, M., 2001. Caspase-11 mediates oligodendrocyte cell death and pathogenesis of autommune-mediated demyelination. J. Exp. Med. 193, 111–122.

Juedes, A.E., Hjelmstrom, P., Bergman, C.M., Neild, A.L., Ruddle, N.H., 2000. Kinetics and cellular origin of cytokines in the central nervous system:

insight into mechanisms of myelin oligodendrocyte glycoprotein-induced experimental autoimmune encephalomyelitis. J. Immunol. 164, 419–426.

Karpus, W.J., Kennedy, K.J., 1997. MIP-1alpha and MCP-1 differentially regulate acute and relapsing autoimmune encephalomyelitis as well as Th1/Th2 lymphocyte differentiation. J. Leukoc. Biol. 62, 681–687.

Kieseier, B.C., Hartung, H.P., 2003. Current disease-modifying therapies in multiple sclerosis. Semin. Neurol. 23, 133–146.

Liedtke, W., Edelmann, W., Chiu, F.C., Kucherlapati, R., Raine, C.S., 1998. Experimental autoimmune encephalomyelitis in mice lacking glial fibrillary acidic protein is characterized by a more severe clinical course and an infiltrative central nervous system lesion. Am. J. Pathol. 152, 251–259.

Louis, J.C., Magal, E., Takayama, S., Varon, S., 1993. CNTF protection of oligodendrocytes against natural and tumor necrosis factor-induced death. Science 259, 689–692.

Luster, A.D., 1998. Chemokines-chemotactic cytokines that mediate inflammation. N. Engl. J. Med. 338, 436–445.

Magnus, T., Rao, M.S., 2005. Neural stem cells in inflammatory CNS diseases: mechanisms and therapy. J. Cell. Mol. Med. 9, 303–319.

Matsumoto, Y., Fujiwara, M., 1993. Immunomodulation of experimental autoimmune encephalomyelitis by Staphylococcal enterotoxin D. Cell. Immunol. 149, 268–278.

Miyagishi, R., Kikuchi, S., Takayama, C., Inoue, Y., Tashiro, K., 1997. Identification of cell types producing RANTES. MIP-1α and MIP-1β in rat experimental autoimmune encephalomyelitis by in situ hybridization. J. Neuroimmunol. 77, 17–26.

Monje, M.L., Toda, H., Palmer, T.D., 2003. Inflammatory blockade restores adult hippocampal neurogenesis. Science 302, 1760–1765.

Namekata, K., Okumura, A., Harada, C., Nakamura, K., Yoshida, H., Harada, T., 2006. Effect of photoreceptor degeneration on RNA splicing and expression of AMPA receptors. Mol. Vis. 12, 1586–1593.

Neuhaus, O., Farina, C., Yassouridis, A., Wiendl, H., Then, B.F., Dose, T., Wekerle, H., Hohlfeld, R., 2000. Multiple sclerosis: comparison of copolymer-1-reactive T cell lines from treated and untreated subjects reveals cytokine shift from T helper 1 to T helper 2 cells. Proc. Natl. Acad. Sci. U.S.A. 97, 7452–7457.

Ohsawa, K., Irino, Y., Nakamura, Y., Akazawa, C., Inoue, K., Kohsaka, S., 2007. Involvement of P2X4 and P2Y12 receptors in ATP-induced microglial chemotaxis. Glia 55, 604–616.

Ponomarev, E.D., Shriver, L.P., Maresz, K., Dittel, B.N., 2005. Microglial cell activation and proliferation precedes the onset of CNS autoimmunity. J. Neurosci. Res. 81, 374–389.

Ralay Ranaivo, H., Craft, J.M., Hu, W., Guo, L., Wing, L.K., Van Eldik, L.J., Watterson, D.M., 2006. Glia as a therapeutic target: selective suppression of human amyloid-β-induced upregulation of brain proinflammatory cytokine production attenuates neurodegeneration. J. Neurosci. 26, 662–670.

Selmaj, K., Raine, C.S., Farooq, M., Norton, W.T., Brosnan, C.F., 1991. Cytokine cytotoxicity against oligodendrocytes. Apoptosis induced by lymphotoxin. J. Immunol. 147, 1522–1529.

Sorensen, T.L., Tani, M., Jensen, J., Pierce, V., Lucchinetti, C., Folcik, V.A., Qin, S., Rottman, J., Sellebjerg, F., Strieter, R.M., Frederiksen, J.L., Ransohoff, R.M., 1999. Expression of specific chemokines and chemokine receptors in the central nervous system of multiple sclerosis patients. J. Clin. Invest. 103, 807–815.

Tanuma, N., Sakuma, H., Sasaki, A., Matsumoto, Y., 2006. Chemokine expression by astrocytes plays a role in microglia/macrophage activation and subsequent neurodegeneration in secondary progressive multiple sclerosis. Acta Neuropathol. 112, 195–204.

Van Der Voorn, P., Tekstra, J., Beelen, R.H., Tensen, C.P., Van Der Valk, P., De Groot, C.J., 1999. Expression of MCP-1 by reactive astrocytes in demyelinating multiple sclerosis lesions. Am. J. Pathol. 154, 45–51.

Vartanian, T., Li, Y., Zhao, M., Stefansson, K., 1995. Interferon-induced oligodendrocyte cell death: implications for the pathogenesis of multiple sclerosis. Mol. Med. 1, 732–743.

Xu, J., Drew, P., 2006. 9-cis-Retinoic acid suppresses inflammatory responses of microglia and astrocytes. J. Neuroimmunol. 171, 135–144.

Zlotnik, A., Yoshie, O., 2000. Chemokines: a new classification system and their role in immunity. Immunity 12, 121–127.

ELSEVIER

Journal of Neuroimmunology 190 (2007) 90–100

Journal of
Neuroimmunology

www.elsevier.com/locate/jneuroim

Characterization of pathogenic T cells and autoantibodies in C-protein-induced autoimmune polymyositis

Yoh Matsumoto *, Kuniko Kohyama, Il-Kwon Park, Mie Nakajima, Keiko Hiraki

Department of Molecular Neuropathology, Tokyo Metropolitan Institute for Neuroscience, Musashidai 2-6, Fuchu, Tokyo 183-8526, Japan

Received 1 August 2007; received in revised form 27 August 2007; accepted 27 August 2007

Abstract

Although autoimmune processes may take place in human polymyositis, little is known with regard to its pathogenesis due to the lack of appropriate animal models. In the present study, we developed experimental autoimmune myositis (EAM) in Lewis rats by immunization with recombinant skeletal C-protein and examined the role of pathogenic T cells and autoantibodies. Using recombinant proteins and synthetic peptides, we demonstrated that skeletal C-protein Fragment 2 (SC2) has the strongest myositis-inducing ability and that myositis-inducing epitope(s) reside within the residues 334–363 of SC2 (SC2P3). However, immunization with SC2P3 induced only mild EAM compared with SC2 immunization. Characterization of T cells and antisera revealed that SC2P3 and SC2P7 contain the B cell epitope, while the T cell epitope resides in SC2P5. Furthermore, anti-SC2, but not anti-SC2P3, antisera contained antibodies against the conformational epitope(s) in the SC2 molecule. However, SC2P3 or SC2P5 immunization plus anti-SC2 antibody transfer aggravated the disease only slightly. These findings suggest that C-protein-induced EAM is formed by activation of C-protein-specific T cells along with antibodies against conformational epitopes in C-protein but that there are undetermined factors related to the disease progression. Further analysis of C-protein-induced EAM will provide useful information to elucidate the pathomechanisms of human polymyositis.

Keywords: Experimental autoimmune myositis; Lewis rat; Protein; Myosin; Immunohistochemistry; B cell epitopes

1. Introduction

Human polymyositis (PM) is a disorder of skeletal muscle characterized by lymphocyte infiltration into the muscle. Immunohistochemical studies of skeletal muscle revealed that T cells are a predominant population of infiltrating inflammatory cells. While CD4-positive T cells were abundant among the surrounding cells, CD8-positive T cells were major invading cells (Arahata and Engel, 1984; Dalakas, 1992; Engel and Arahata, 1984). These findings suggest that PM is an autoimmune disease. However, little is known regarding its pathogenesis partly because a good animal model for PM is not available at present. In previous studies, we and others induced experimental autoimmune polymyositis (EAM) in Lewis rats by immunization with partially purified skeletal myosin (Kojima et al., 1997; Nemoto et al., 2003). During the process of subsequent investigations, we found that immunization with myosin that had been further purified from partially purified myosin preparations induced only mild EAM compared with partially purified myosin-induced EAM. Moreover, immunization with purified C-protein, a myosin-binding protein (Offer, 1972; Offer et al., 1973), induced severe EAM of high histological grade and lesion frequency comparable with EAM induced with partially purified myosin. These findings suggested that C-protein is the major myositogenic antigen that exists in the partially purified myosin preparation (Kohyama and Matsumoto, 1999).

C-protein is a single polypeptide chain of approximately 140 kDa, which is present in thick filaments of skeletal and cardiac muscles. It binds to myosin rods, light meromyosin, and F-actin (Dennis et al., 1984). Although its function is not fully

Abbreviations: EAM, experimental autoimmune myositis; PM, polymyositis; SC2, skeletal muscle C-protein fragment 2; SC2P3, SC2 peptide 3.

* Corresponding author. Tel.: +81 423 25 3881x4719; fax: +81 423 21 8678.
E-mail address: matyoh@tmin.ac.jp (Y. Matsumoto).

0165-5728/$ - see front matter © 2007 Elsevier B.V. All rights reserved.
doi:10.1016/j.jneuroim.2007.08.013

understood, C-protein seems to encircle each thick filament and to play an important role in stabilizing the thick filament structure (Fischman et al., 1991). C-protein is a member of the immunoglobulin super family and has several isoforms and different isoforms have characteristic distributions (Dennis et al., 1984).

Analysis of EAM using native C-protein purified from skeletal muscle has several limitations. Firstly, C-protein comprises only 2% of muscle proteins and therefore it is difficult to perform experiments using a large amount of the protein (Offer, 1972; Offer et al., 1973). Secondly, further investigation with native C-protein revealed that the purity and myositogenicity of the protein varied greatly from lot to lot, resulting in variation in the induction of EAM. Finally and most importantly, fine specificity analysis was difficult due to its large molecular size.

To overcome these problems, we have prepared, in the present study, recombinant skeletal C-protein fragments (SC1–SC4) and overlapping synthetic peptides corresponding to one of the fragments (SC2). Analysis of the T and B cell epitopes revealed that the T epitope resides within peptides 5 (SC2P5), whereas anti-SC2 antibodies react with SC2P3 and SC2P7. Furthermore, it was suggested that full-blown EAM is induced by synergistic effects by T cells and antibodies responding these epitopes. Thus, the animal model established in the present study will provide useful information to analyze the pathomechanisms and to develop specific immunotherapy for human PM.

2. Materials and methods

2.1. Animals

Lewis rats were purchased from SLC Japan (Shizuoka) and bred in our animal facility. Rats used in the present study were 8–12 weeks old. All the experiments performed in the present study were approved by Ethical Committee of Tokyo Metropolitan Institute for Neuroscience.

2.2. C-protein purification

C-protein was isolated from partially purified myosin. The C-protein-containing fraction was concentrated and dialyzed against 0.3 M KCl, 0.01 M potassium phosphate (pH 7.0) with 0.01% sodium azide. Hydroxyapatite column chromatography was performed according to Starr and Offer (1982) with a few modifications. The sample was applied to a 1.6 × 15 cm column of hydroxyapatite (Calbiochem, Tokyo, Japan) and eluted with potassium phosphate pH7.0 (0.01–0.5 M linear gradient) to obtain purified C-protein, which was present in approximately 0.15 M potassium phosphate.

Detection of C-protein was performed by polyacrylamide gel electrophoresis, which revealed the protein as a band of about 140 kDa. This was also confirmed by western blotting with anti-C-protein mAb. To determine the purity of C-protein obtained, 1 μg of the protein was run on a gradient PAGE (5–20%) (Biocraft, Tokyo, Japan) and the gel was stained with SYPRO Red (Molecular Probes, Eugene, OR) for 30 min. Then, the profiles were recorded using an FMBIO II fluorescence image analyzer (Hitachi, Yokohama, Japan). The percentage of C-protein was calculated as the percentage of the density of a band of 140 kDa per the density of the total protein.

2.3. Preparation of recombinant C-protein fragments

Since C-protein (140 kDa) is too large to prepare the recombinant protein as a whole protein, we planned to produce four protein fragments designated as Fragments 1, 2, 3, and 4 as shown in Fig. 1. Total RNA was isolated from human psoas muscle using RNAzol B (Biotecx Laboratories, Houston, TX)

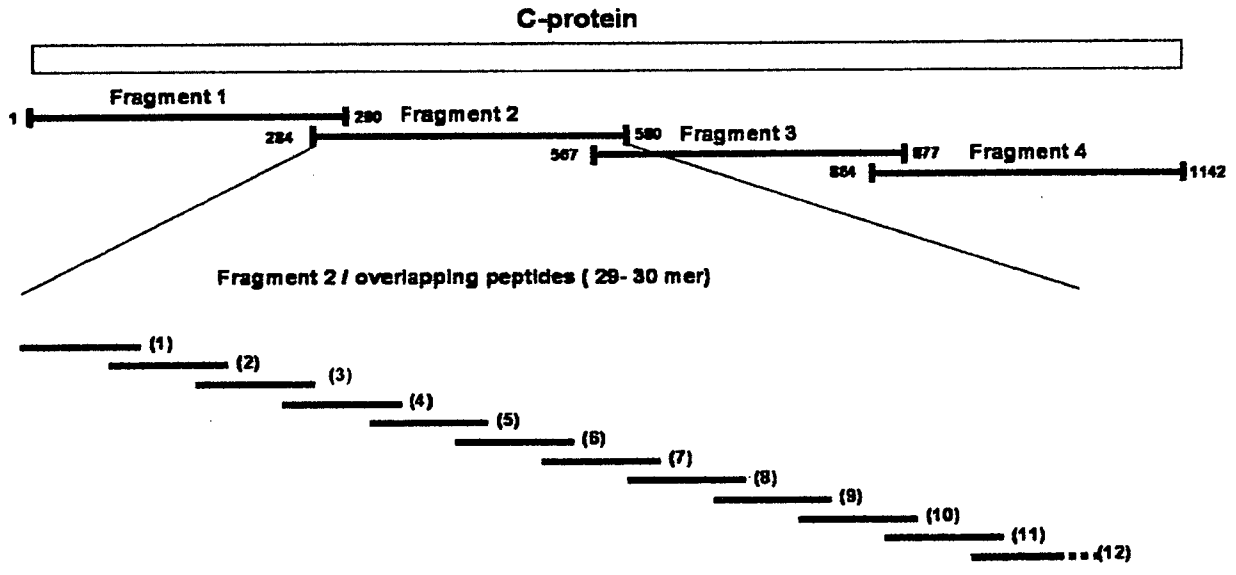

Fig. 1. Recombinant C-protein and synthetic peptides used in this study. Four recombinant protein fragments corresponding to residues 1–290, 284–580, 567–877 and 864–1142 of C-protein were prepared from transformed *E. coli* and purified with an affinity column. Twelve overlapping 29–30 mer synthetic peptides covering Fragment 2 were also prepared for immunization and in vitro proliferation assay.

and then reverse transcribed into cDNA using ReverTra Ace-α- (TOYOBO, Osaka, Japan). Then, cDNA was amplified by PCR with KOD DNA polymerase (TOYOBO) and fragment-specific primer pairs. Primers used in this study were as follows: Fragment 1 (sense primer=5′-GAGAGGTACCATGCCT-GAGGCAAAACCAGCG-3′, antisense primer=5′-GAGAGTCGACTCAGAACCACTTGAGGGTCAGGTC-3′); Fragment 2 (sense primer=5′-GAGAGGATCCGACCT-GACCCTCAAGTGGTTC-3′, antisense primer=5′-GAGAAA-GCTTCAGCCAGGTAGCGACGGGAGG-3′); Fragment 3 (sense primer=5′-AGAGGATCCCCTCCCGTCGCTACCT-GGCTG-3′, antisense primer=5′-AGAAAGCTTCC-GGGGCTTTCCCTGGAAGGG-3′) and, Fragment 4 (sense primer=5′-AGAGGATCCCCCTTCCAGGGAAAGCCCCGG-3′, antisense primer=5′-AGAAAGCTTTCACTGCGG-CACTCGGACCTC-3′). Each primer was designed to introduce the restriction enzyme sites at both ends. PCR products were inserted into a cloning vector, pCR4 Blunt-TOPO in the Zero Blunt TOPO kit (Invitrogen, CH Groningen, the Netherlands), and clones with the correct sequences were obtained by the standard method. Several clones were subcloned into an expression vector, pQE30 (QIAGEN, Tokyo, Japan), and used for large-scale preparation of C-protein fragments. Recombinant C-protein fragments produced in transformed *E. coli* were isolated under denaturing conditions and purified using Ni-NTA Agarose (QIAGEN). Then, purified protein fragments were refolded in 100 mM PBS containing 500 mM L-arginine, 2 mM glutathione (reduced form), 0.2 mM glutathione (oxidized form), and 2 mM EDTA. As a final step, recombinant protein fragments were incubated with Detoxi-Gel (PIERCE, Funakoshi, Tokyo, Japan) overnight to remove endotoxins. Obtained protein fragments contained endotoxins less than 10 EU/1 mg protein as determined with Toxinometer ET-2000 (Wako, Tokyo, Japan).

Overlapping 29–30 mer synthetic peptides covering C-protein Fragment 2 (SC2) were synthesized using a peptide synthesizer (PSSM-8, Shimadzu, Kyoto, Japan) and designated as SC2P1-P12 (Fig. 1). All the peptides used in this study were >90% pure, as determined, and purified if necessary, by HPLC.

2.4. EAM induction and tissue sampling

Lewis rats were immunized by intramuscular injections of the indicated antigen with complete Freund adjuvant (CFA) (Gibco, Tokyo, Japan) in multiple sites of the back three times on a weekly basis, and were sacrificed two weeks after the last immunization. For controls, PBS/CFA was injected according to the same protocol. Where indicated, *M. tuberculosis* (Gibco) was further supplemented to 5 mg/ml (5CFA). To prevent degeneration of the antigens, only freshly prepared or short-term preserved (one month or less at −80 °C) preparations were used for experiments. At the time of immunization, rats received an intraperitoneal injection of 2 μg pertussis toxin (PT) (Seikagakukogyo, Tokyo, Japan). Histological and immunohistochemical examinations were performed using frozen sections of muscle that had been removed from a proximal part of lower extremities (total six blocks) and snap frozen in chilled isopentane precooled in liquid nitrogen.

2.5. Histological grading of inflammatory lesions and immunohistochemistry

Using hematoxylin and eosin-stained sections, histological severity of inflammation was graded into four categories: grade 1, single or less than 5 muscle fiber involvement; grade 2, a lesion involving 5–30 muscle fibers; grade 3, a lesion involving a muscle fasciculus; grade 4, a diffuse extensive lesion. When multiple lesions were found in one muscle block, 0.5 was added to the score.

ATPase staining was performed to distinguish fast (white) muscle fibers from slow (red) muscle fibers. Frozen sections were treated with barbital acetate solution, 0.1 M HCl (pH 4.6) for 5 min after which the sections were washed in 0.1 M sodium barbital, 0.18 M $CaCl_2$ (pH 9.5). Then, sections were reacted with ATP disodium salt in sodium barbital solution for 45 min. The reaction products were visualized in 1% ammonium sulfide solution (yellow).

Immunoperoxidase staining was performed as described (Matsumoto et al., 1986). Briefly, frozen sections, 10 μm thick, were air-dried and fixed in ether for 10 min. After incubation with normal sheep serum, sections were allowed to react with mAb, biotinylated horse anti-mouse Ig (1:200) (Vector, Burlingame, CA) and horseradish peroxidase (HRP)-labeled VECTASTAIN® *Elite* ABC Kit (Vector). HRP-binding sites were detected using a Sigma Fast DAB Tablet set (Sigma). The monoclonal antibodies (mAb) in the present study were R73 (1:800) (anti-T cell receptor αβ), OX42 (1:400) (anti-macrophage), W3/25 (1:400) (anti-CD4), and clone 341 (1:200) (anti-CD8). The mAbs were purchased from Serotec (Blackthorn, Bicestor, Bucks, UK) or purified from culture supernatant of hybridomas. Immunohistochemical staining with anti-SC2 mAbs, which were raised using recombinant SC2 protein, was also performed to test whether the mAbs react with native protein. To confirm the specificity, the mAbs were absorbed by incubating with 10 M excess of recombinant SC2 for 1 h at 37 °C and immunohistochemistry was performed.

2.6. Proliferative responses of T cells against SC2 and SC2 peptides

Proliferative responses of lymph node cells were assayed in microtiter wells by uptake of $\{^3H\}$-thymidine. After being washed with PBS, lymph node cells (2×10 cells/well) were cultured with the indicated concentrations of SC2 or SC2 peptides for 3 days, with the last 18 h in the presence of 0.5 μ Ci $\{^3H\}$ thymidine (Amersham Pharmacia Biotech, Tokyo). In some experiments, the proliferative responses of SC2 or SC2 peptide-specific T line cells (3×10^4 cells/well) were assayed in the presence of the antigens and APC (5×10^5 cells/well). The cells were harvested on glass-fiber filters, and the label uptake was determined using standard liquid scintillation techniques.

2.7. ELISA and western blot analysis

The levels of anti-SC2 and anti-SC2 peptide antibodies were measured by ELISA. Recombinant SC2 and SC2 peptides

Table 1
Induction of experimental autoimmune myositis with native C-protein preparations

Immunization[a]		Incidence[b]	% inflammatory lesion[c]	Histological score[d]
Native C-protein	Purity[e]			
Lot #6	52%	7/7	35/42 (83%)	1.9±1.0
Lot #7	68%	3/8	8/48 (17%)	0.9±0.4
Lot #8	42%	3/4	7/24 (29%)	0.9±0.4
Lot #9	38%	3/3	12/18 (67%)	1.0±0.2

[a] Lewis rats were immunized with the indicated lot of native C-protein in CFA along with pertussis toxin and sacrificed one week after the last immunization. Muscles in the hind feet were removed (6 blocks) and snap frozen in chilled isopentane. Histological severities were graded in four categories: grade 1, single or less than 5 lesions involving 1–5 muscle fiber(s); grade 2, single lesion involving 5–30 muscle fibers or single muscle fasciculus; grade 3, single lesion involving 1–10 muscle fasciculus; grade 4, a diffuse extensive lesion.

[b] When inflammation was found in at least one site on hematoxylin and eosin-stained sections, rats were scored as positive.

[c] No. of muscle blocks containing inflammatory foci/No. of total blocks examined.

[d] Total histological scores/No. of blocks examined±SE.

[e] The purity of each C-protein preparation was determined as follows. Each lot of C-protein was run on a gradient PAGE and stained with SYPRO Red. Then, the profiles were recorded using an FMBIO II fluorescence image analyzer. The percentage of C-protein was calculated as the percentage of the density of a band of 140 kDa per the density of the total protein.

(10 μg/ml) were coated onto microtiter plates and serially diluted sera from normal and immunized animals were applied. After washing, appropriately diluted horseradish-conjugated anti-rat IgG, IgG1, or IgG2a was applied. The reaction products were then visualized after incubation with the substrate. The absorbance was read at 450 nm.

For the immunoblot assay, SC2 was run on a 10% SDS-PAGE gel and immunoblotted onto nitrocellulose membrane (Bio-Rad, Hercules, CA). The residual binding sites on the membrane were blocked by incubation with 5% nonfat milk in TBS buffer (10 mM Tris–HCl, pH 7.4, and 150 mM NaCl) for 1 h and then incubated with anti-SC2 mAb for 2 h. The blots were washed three times in TBS containing 0.1% Tween-20, probed with horseradish peroxidase-conjugated anti-mouse IgG (New England Biolabs, Inc, Beverly, MA) for 1 h. The blots were developed by enhanced chemiluminescence reagents (Amersham Life Science, Arlington Heights, IL) according to the manufacturer's instructions. The density of each band obtained by western blot analysis was measured with a scanning laser densitometer (GS-700, Bio-Rad, Hercules, CA) and analyzed using Molecular Analyst software (Bio-Rad, Hercules, CA).

2.8. Purification of sera with SC2- or SC2 peptide-coupled column

SC2- or SC2 peptide-coupled affinity columns were prepared using HiTrap NHS-activated columns (GE Healthcare, Bioscience Corp, Tokyo, Japan) according to the manufacturer's instructions. SC2 was dialyzed in the standard coupling buffer (0.2 M $NaHCO_3$, 0.5 M NaCl, pH 8.3) and the SC2 peptide mixture (SC2P1–SC2P12) was dissolved in dH_2O containing 1% DMSO and 1% PBS. SC2 or peptide mixture was coupled to the column as a ligand. Then, sera obtained from EAM-induced rats were fractionated on SC2- or SC2 peptides-coupled columns. Briefly, the sera were diluted five-fold with PBS and applied to the column that had been equilibrated with 20 mM Na–PO_4, pH 7. After the flowthrough was saved, the column was washed and the bound protein was eluted with 0.1 M glycine–HCl, pH 2.7 and immediately neutralized with 1 M Tris–HCl, pH 9. The levels of anti-SC2 and anti-SC2 peptide antibodies in the flowthrough and eluate were determined by ELISA.

2.9. Generation of monoclonal and polyclonal antibodies against SC2 and SC2 peptides and transfer experiments

Anti-SC2 and anti-SC2P3 mAbs were generated by immunizing Balb/C mice (SLC, Shizuoka, Japan) with SC2 and SC2P3, respectively. To increase the immunogenicity of SC2P3, the peptide was conjugated with keyhole limpet hemocyanin (KLH) (Wako, Tokyo, Japan) before use. Mice were first immunized with 50 μg antigens emulsified with CFA followed by intraperitoneal injections of antigens/IFA in a total of six times. The sufficient production of antibodies was confirmed by ELISA using sera obtained by retro-orbital puncture. After the final boost, spleen cells taken from immunized mice were hybridized with myeloma cells (X63Ag8.653) using polyethylene glycol (PEG/DMSO solution Hybri-Max, Sigma, Tokyo, Japan). After seeding onto microplates, hybridoma cells were selected in the HAT medium. Ten to fourteen days later, antibody-producing cells were screened by ELISA and cloned by limiting dilution. Established clones were expanded in culture and cells were injected intraperitoneally to Balb/C mice with Pristane (Sigma) to obtain a large amount of mAbs. The mAbs obtained was purified on a HiTrap protein G column (Amersham Bioscience, Tokyo, Japan). Anti-SC2 rat mAbs were also generated in a similar way. In this case, Lewis rats were immunized with SC2 and sacrificed 2 weeks

Table 2
Histological severities of EAM induced by immunization with recombinant skeletal C-protein fragments[a]

Antigen	Incidence[b]	% inflammatory lesion[c]	Mean histological score[d]
SC1	4/4	13/24 (63%)	0.83±0.20
SC2	9/9	35/54(65%)	1.36±0.18
SC3	6/6	17/35 (51%)	1.09±0.23
SC4	2/3	6/18 (39%)	0.56±0.20
PBS	2/3	2/19 (11%)	0.11±0.08

a) Lewis rats were immunized with recombinant C-protein fragment 1, 2, 3, or 4 (SC1, SC2, SC3 and SC4, respectively) in CFA along with pertussis toxin and sacrificed one week after the last immunization. PBS/CFA-immunized controls showed non-specific single muscle fiber necrosis in two of three rats. Therefore, such finding was not judged as positive in SC-immunized animals.
b) When inflammation was found in at least one site on hematoxylin and eosin-stained sections, rats were scored as positive.
c) No. of muscle blocks containing inflammatory foci/No. of total blocks examined.
d) Total histological scores/No. of blocks examined±SE.
e) Significantly different between SC1 and PBS ($p<0.01$), between SC2 and PBS ($p<0.001$), between SC3 and PBS ($p<0.01$), and between SC4 and PBS ($p<0.05$) by Student's t test.

after immunization. Iliac lymph node cells were taken from the rats and hybridized with myeloma cells, SP2/0-Ag14, kindly provided by Dr. Sado (Shigei Medical Research Institute, Okayama, Japan).

Polyclonal antibodies against SC2 and SC2 peptides were raised by immunizing rats with the antigens/CFA four times on a weekly basis. Sera were obtained one week after the last immunization and ammonium sulfate-precipitated preparations were used for the transfer experiments. The presence of antibodies against the indicated antigens was confirmed by ELISA.

For the transfer experiments, rats were first immunized with SC2 peptide and the indicated doses of sera or mAb were injected intravenously twice a week for 3 weeks. Rats were examined histologically 2 weeks after the last antibody administration.

2.10. Statistical analysis

Unless otherwise indicated, Student's t test or Mann–Whitney's U-test was used for the statistical analysis.

3. Results

3.1. Purity and myositogenicity of native C-protein purified from skeletal muscle varied from lot to lot of the protein

In a previous report (Kohyama and Matsumoto, 1999), we showed that immunization with purified native C-protein induced severe EAM in Lewis rats comparable with that induced with partially purified skeletal myosin (Kojima et al.,

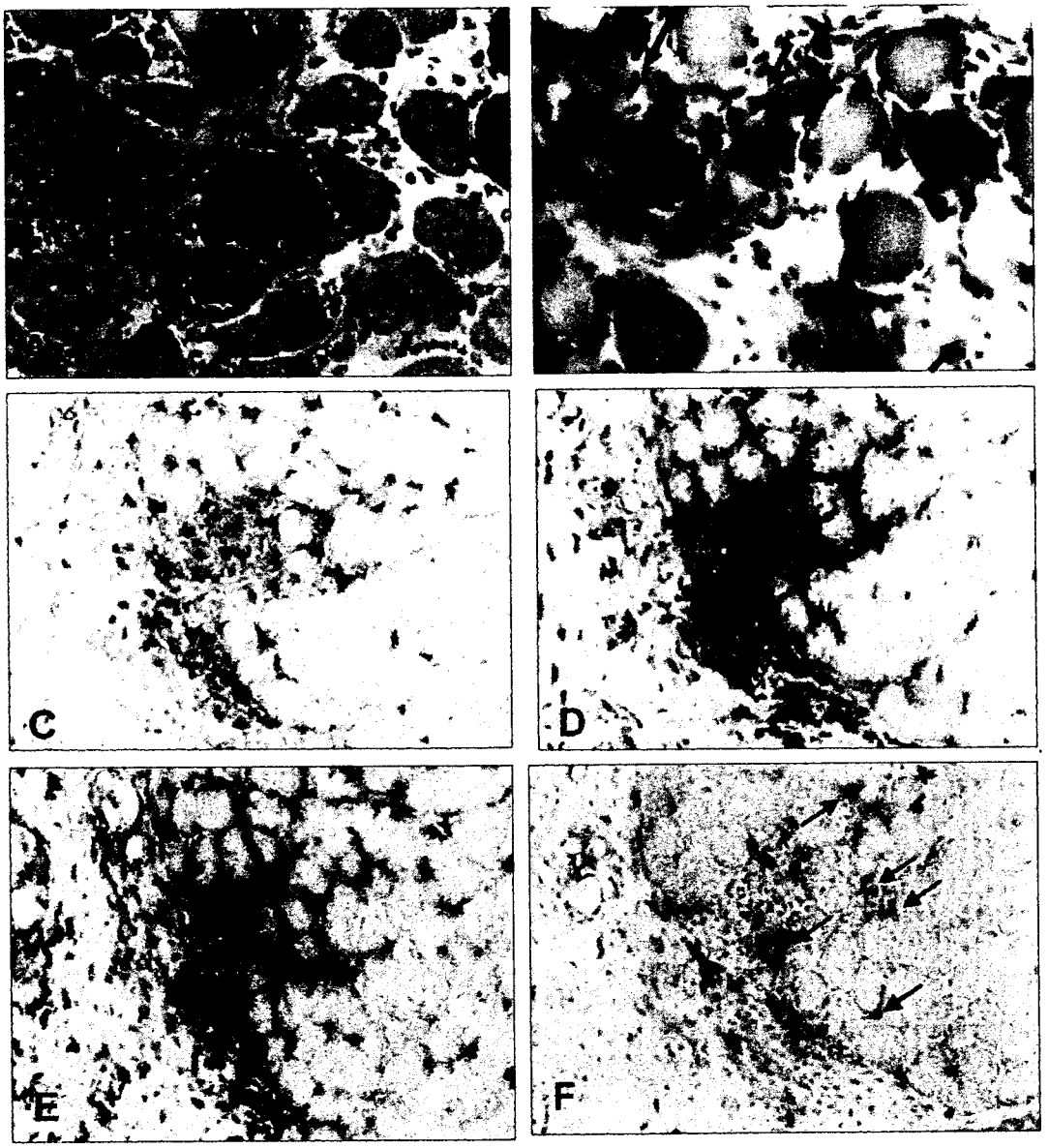

Fig. 2. Immunopathology of C-protein-induced EAM. In H and E staining (A), inflammatory cells infiltrated muscle fibers (one of the residual fibers is indicated by arrow heads) and the perimysial space is filled with infiltrating cells. ATPase staining (B) revealed that white muscle fibers (light staining and indicated by arrows) are attacked by inflammatory cells, whereas red muscle fibers (dark staining and indicated by arrow heads) are relatively spared from inflammation. Immunoperoxidase staining demonstrated that TCR αβ-positive T cells (C) and macrophages (D) have mainly infiltrated the lesion. Although CD4-positive cells (E) outnumber CD8-positive cells (F), CD8-positive cells infiltrated the muscle fibers (arrows in F).

1997). In contrast, highly purified myosin induced only mild EAM. These findings suggested that the major myositogenic component in the partially purified myosin preparation is C-protein. To characterize C-protein-induced EAM in more detail, we repeated the experiments using new lots of native C-protein. Unexpectedly, however, the purity and myositogenicity of purified native protein varied from lot to lot, as summarized in Table 1. All the rats (7 out of 7) that had received Lot #6 developed severe EAM with a mean histological score of 1.9 in 35 muscle blocks out of 42 blocks examined. In contrast, Lots #7 and #8 induced only mild EAM with histological scores of 0.9 in 17–29% of muscle sections. It should be noted that the purity of C-protein in each lot did not always correlate with myositogenicity. For instance, Lot #7 with relatively high purity (68%) induced mild EAM, while Lot #9 with low purity (38%) induced intermediate EAM (Table 1). This was probably because myositogenicity of purified native C-protein is related not only to the purity of C-protein, but also to the preservation of the intact protein after purification.

3.2. Incidence and immunopathology of recombinant C-protein-induced EAM

To overcome the above problems and to obtain a sufficient amount of C-protein with high purity, we decided to prepare recombinant proteins. Since C-protein is too large to produce a plasmid encoding the whole sequence of the protein, we prepared four plasmids encoding four parts of fast-type C-protein as shown in Fig. 1. Fragments 1, 2, 3, and 4 (referred to as SC1, SC2, SC3, and SC4) correspond to residues 1–290, 284–580, 567–877, and 864–1142, respectively. Then, purified recombinant protein fragments were immunized three times on a weekly base into Lewis rats, and muscle blocks were taken two weeks after the last immunization for histological examination. The results are summarized in Table 2. Immunization with SC1, SC2, SC3, and SC4 induced EAM in all rats. Control rats that were immunized with PBS/CFA showed mild non-specific inflammation in the muscle with very low incidence compared with C-protein-immunized rats (Table 2). We have checked the site of inflammation in PBS/CFA-immunized rats and found that inflammation was far from the immunization site. Therefore, it is unlikely that inflammation was tissue damage directly induced by adjuvant. Among the C-protein-immunized groups, SC2 induced severe EAM with mean histological severity of 1.36±0.18 in 65% of muscle tissue blocks comparable with partially purified myosin-induced or native C-protein-induced EAM (Kohyama and Matsumoto, 1999). Similarly, SC3 induced intermediate EAM. Immunization with SC1 and SC4 resulted in relatively mild EAM in terms of incidence and severity. These findings indicate that in the C-protein molecule, there are multiple myositis-inducing epitopes.

Histological examination revealed severe inflammatory cell infiltration into muscle fibers (Fig. 2A). In ATPase staining, inflammatory cells comprising T cells and macrophages mainly infiltrated fast-type fibers (Fig. 2B, arrows) and slow-type fibers

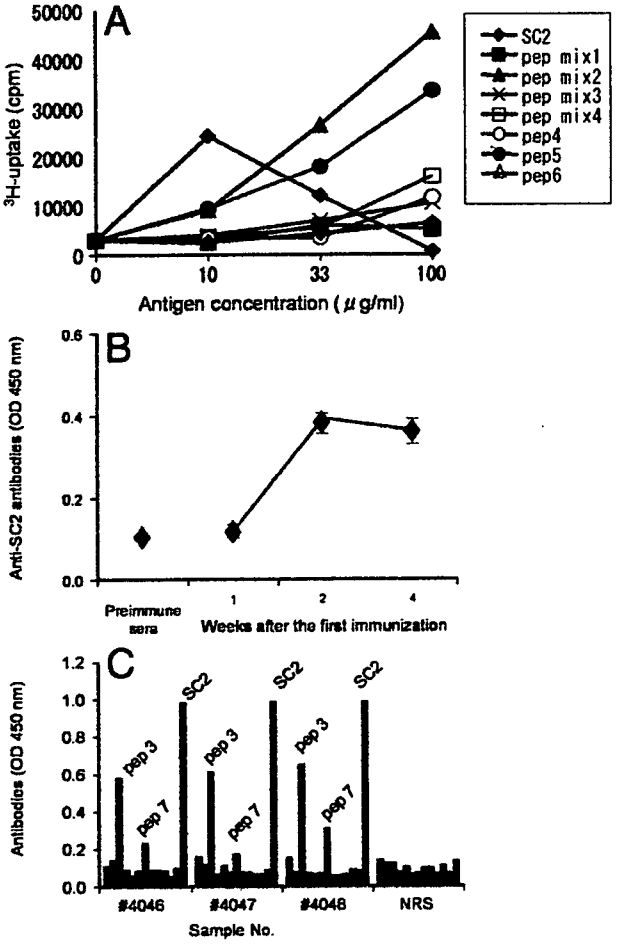

Fig. 3. Characterization of T cells and autoantibodies in SC2-induced EAM. A; Proliferative responses of lymph node cells taken from SC2-immunizaed rats respond vigorously to Mix 2 (SC2P4, P5 and P6, closed triangles) and pep5 (SC2P5, closed circles). Lymph node cells also react with the immunogen, SC2 (closed diamonds). B; Kinetics of anti-SC2 antibody titer during the course of EAM. The level of anti-SC2 antibodies increased and reached a maximum two weeks after the first immunization. Sera were taken from the same animals at various time points. C; The reactivities of anti-SC2 antisera to overlapping synthetic peptides encompassing SC2. All the sera taken from SC2-immunized rats 4 weeks after the first immunization reacted with peptide 3 (SC2P3) and, to lesser extent, to peptide 7 (SC2P7). NRS, normal rat serum.

Table 3
Sequences of SC2[a] peptides used in the study

Peptide	Residue	Sequence
SC2P1	SC284–313	DLTLKWFKNGQEIKPSSKYVFENVGKKRIL
SC2P2	SC309–338	KKRILTINKCTLADDAAYEVAAYEVKCFTE
SC2P3	SC334–363	KCFTELFVKEPPVLIVTPLEDQQVFVGDRV
SC2P4	SC359–388	VGDRVEMAVEVSEEGAQVMWMKDGVELTRE
SC2P5	SC384–412	ELTREDSFKARYRFKKDGKRHILIFSDVV
SC2P6	SC408–436	FSDVVQEDRGRYQVITNGGQCEAELIVEE
SC2P7	SC432–460	LIVEEKQLEVLQDIADLTVKASEQAVFKC
SC2P8	SC456–484	AVFKCEVSDEKVTGKWYKNGVEVRPSKRI
SC2P9	SC480–508	PSKRITISHVGRFHKLVIDDVRPEDEGDY
SC2P10	SC504–532	DEGDYTFVPDGYALGSLSAKLNFLEIKVE
SC2P11	SC528–556	EIKVEYVPKQEPPKIHLDCSGKTSENAIV
SC2P12	SC552–572[b]	ENAIVVVAGNKLRLDVSITGE

[a] Amino acid residues 284–580 of human skeletal C-protein, fast type.
[b] Amino acid residues 573–580 (PPPVATWL) were deleted because the sequence was difficult to synthesize.

Table 4
Histological severities of EAM induced by immunization with synthetic peptides[a]

Group	Antigen	Dose (μg)	Incidence[b]	% inflammatory lesion[c]	Mean histological score[d]
A	SC2	100/cCFA[e]	9/9	35/54 (65%)	1.36±0.18[f]
B	SC2P1	100/cCFA	2/3	3/18 (17%)	0.17±0.09
C	SC2P2	100/cCFA	2/3	2/18 (11%)	0.11±0.08
D	SC2P3	100/cCFA	3/3	7/18 (39%)	0.42±0.13
E	SC2P4	100/cCFA	1/3	2/18 (11%)	0.11±0.08
F	SC2P5	100/cCFA	1/3	1/18 (6%)	0.06±0.06
G	SC2P6	100/cCFA	3/3	3/18 (17%)	0.17±0.09
H	SC2P7	100/cCFA	1/3	1/18 (6%)	0.06±0.06
I	SC2P8	100/cCFA	2/3	3/18 (17%)	0.17±0.09
J	SC2P9	100/cCFA	3/3	4/18 (22%)	0.22±0.10
K	SC2P10	100/cCFA	2/2	4/12 (33%)	0.25±0.12
L	SC2P11	100/cCFA	3/3	5/18 (28%)	0.19±0.08
M	SC2P12	100/cCFA	1/2	2/12 (17%)	0.13±0.09
N	PBS	PBS/cCFA	2/3	2/18 (11%)	0.11±0.08

[a] Lewis rats were immunized with the indicated C-protein peptide in CFA along with pertussis toxin and sacrificed one week after the last immunization. Three rats per each peptide except for SC2P11 were immunized and examined histologically. The results for SC2 (Group A) and controls (Group N) listed in Table 2 are shown again for comparison.

[b] When inflammation was found in at least one site on hematoxylin and eosin-stained sections, rats were scored as positive.

[c] No. of muscle blocks containing inflammatory foci/No. of total blocks examined.

[d] Total histological scores/No. of blocks examined±SE.

[e] cCFA, conventional CFA containing 1 mg/ml *M. tuberculosis*.

[f] Significant differences were noted between the following two groups; A vs. J ($p<0.01$) and D vs. J ($p<0.05$).

were relatively spared (Fig. 2B, arrowheads). Since homology between fast-type and slow-type C-protein at the amino acid level is low (49.5% based on the NCBI database), it is possible that T cells activated by immunization with fast-type C-protein recruited mainly to fast-type fibers and not to slow-type fibers. Immunohistochemical examination demonstrated that predominant populations of infiltrating cells were αβ T cells (Fig. 2C) and macrophages (Fig. 2D) and that the number of γδ T and NK cells was small (data not shown). CD4 staining showed that the number and distribution of CD4-positive cells are almost the same as those of macrophages (Fig. 2E) because the CD4 molecules are expressed on both T cells and macrophages in rats (Jefferies et al., 1985). The number of CD8-positive cells was relatively small and CD4:CD8 ratio was 2.5±0.2. However, many of the CD8-positive cells were found at the interface of inflammation and remaining muscle fibers (Fig. 2F) and some were infiltrating muscle fibers (arrows in Fig. 2F), suggesting the importance of this cell type in lesion formation. These immunopathological findings are essentially the same as those found in native C-protein-induced EAM and human PM, implying that recombinant C-protein-induced EAM can serve as a model for human PM.

3.3. T and B cell epitopes in SC2-induced EAM

In order to characterize T and B cell epitopes, we focused on SC2 for further analysis for two reasons. First, SC2 showed high myositogenicity as demonstrated in Table 2. In addition, SC2 was hydrophilic, while SC3, which also showed intermediate myositogenicity, was hydrophobic and almost insoluble in water. Therefore, SC2 was more suitable for in vitro studies than SC3. For further analysis, we also produced overlapping synthetic peptides covering the SC2 molecule (Fig. 1 and Table 3). To identify T cell epitope(s), we next examined the proliferative responses of lymph node T cells taken from SC2-immunized animals (Fig. 3A). To screen the candidate peptide(s), peptide mixtures designated as Mix 1, 2, 3, and 4 were prepared. The mixtures contained 1–3, 4–6, 7–9, and 10–12, respectively.

A pilot study suggested that Mixture 2 contains T cell epitope (s). As clearly shown in Fig. 3A, Mixture 2 and immunizing protein, SC2, induced strong responses of T cells from SC2-immunized rats, while Mixtures 1, 3, and 4 induced only marginal responses. In a parallel assay, it was demonstrated that SC2P5, but not SC2P4 or SC2P6, in Mix 2 was responsible for T cell proliferation (Fig. 3A). We repeated the assays three times and obtained essentially the same results. Thus, it was clearly

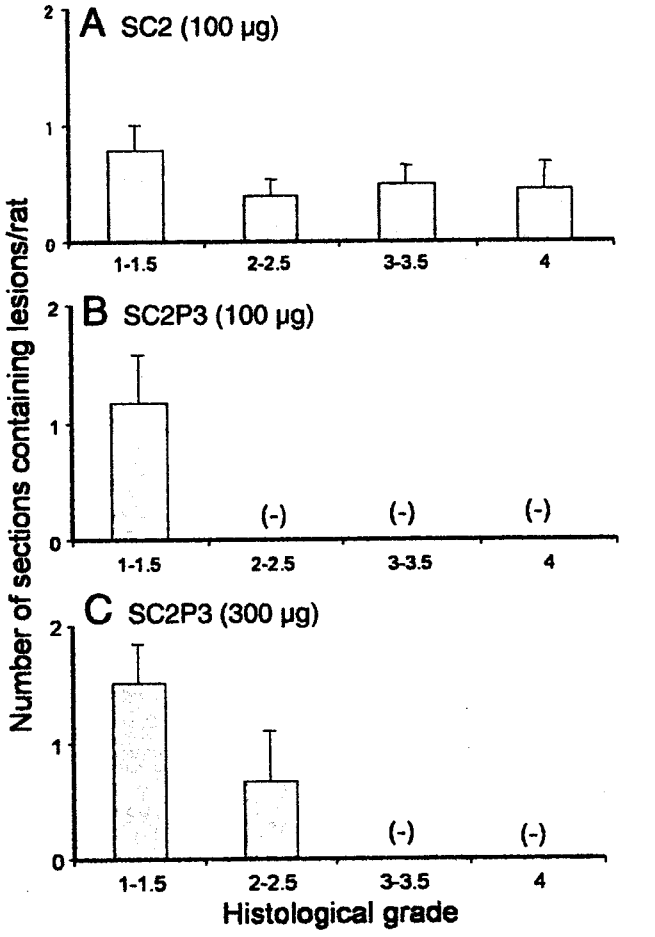

Fig. 4. Histological severities of muscle inflammation induced by immunization with SC2 (A), SC2P3 (100 μg) (B), and SC2P3 (300 μg) (C). The histological severities of EAM induced by three different immunogens were analyzed semiquantitatively. In SC2-induced EAM, rats developed almost equal proportions of Grade 1–4 lesions (A), whereas SC2P3-immunization induced only mild EAM (B). Increase of the immunogen resulted in the production of Grade 2–2.5 lesions, but not of Grade 3–4 lesions.

demonstrated that SC2P5 contains the T cell epitope. However, non-responder peptides could contain T cell epitope(s) because there is the possibility that long peptides used in the proliferation assay may not be properly processed and presented by APC.

Then, the B cell epitopes were determined using sera taken from SC2-immunized rats. As shown Fig. 3B, the level of anti-SC2 antibodies was elevated two weeks after the first immunization and reached a plateau thereafter. At four weeks after the first immunization, anti-SC2 antibodies reacted with SC2P3, and to lesser extent with SC2P7, in all the cases examined (Fig. 3C).

3.4. Identification of myositogenic epitopes in C-protein Fragment 2

Each peptide was immunized at a dose of 100 μg into rats and the results are summarized in Table 4. As clearly shown in Group D, SC2 Peptide 3 (SC2P3) exhibited the strongest myositogenicity in terms of the incidence (3/3), % inflammatory lesion (39%) and histological score (0.42±0.13) among 12 peptides tested. Immunization with other peptides induced no or marginal pathology compared with the PBS control. Although SC2P5 and SC2P7 contain T and B cell epitope, respectively, as shown in previous experiments, they did not show significant myositogenicity. Since SC2P3 induced mild EAM with this immunization protocol compared with SC2, we further tested its EAM-inducing ability with a stronger protocol. Immunization with SC2P3 at a higher dose (300 μg) emulsified in CFA containing *M. tuberculosis* at 5 mg/ml (5CFA) induced more severe EAM (1.03±0.32) with a higher frequency of inflammatory lesions (72%). However, there was still clear difference in histopathology between SC2P3- and SC2-induced EAM. Since we felt that in SC2P3-induced EAM, mild lesions were found more frequently than in SC2-induced EAM, we counted the number of lesions categorized in Scores of 1–1.5, 2–2.5, 3–

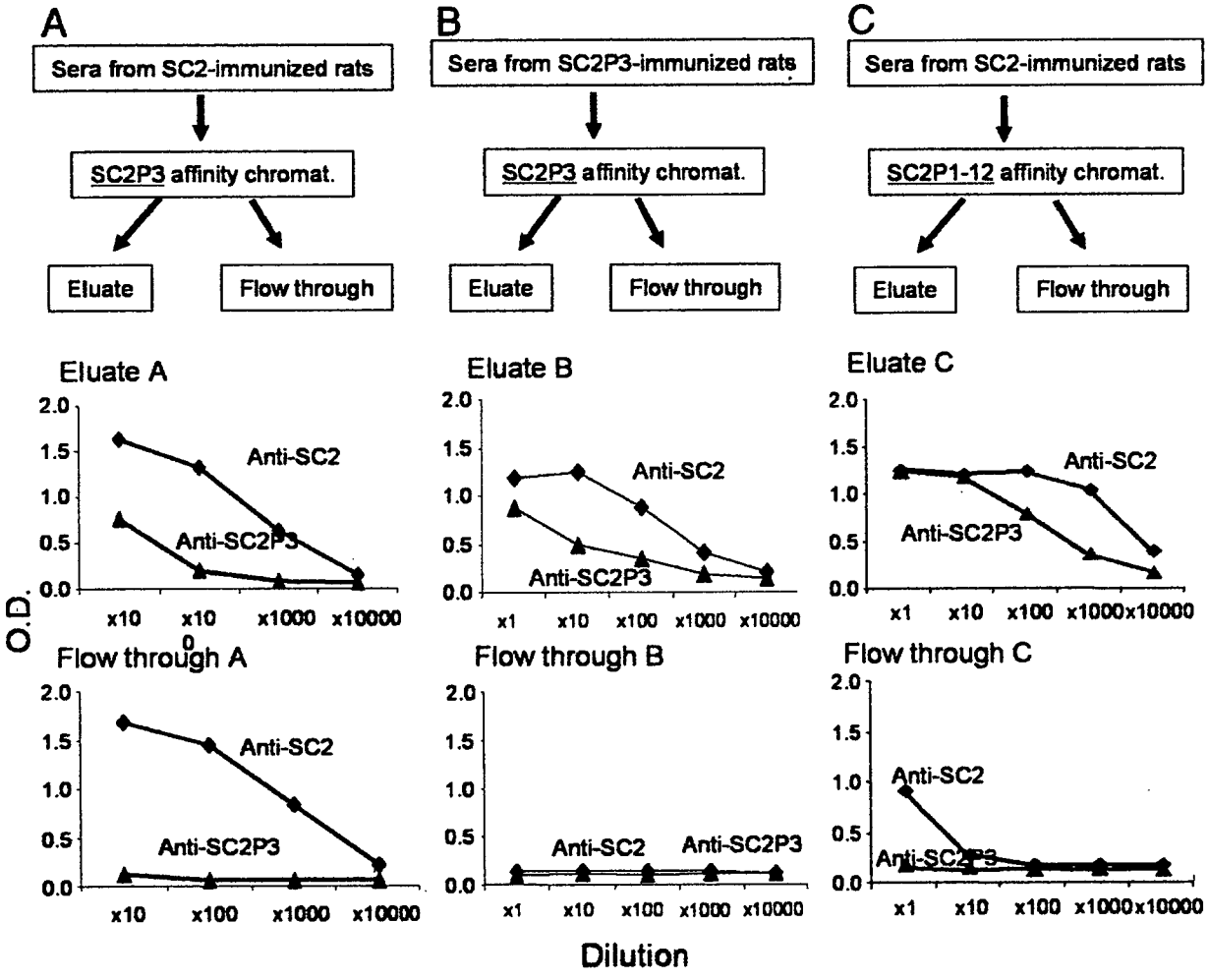

Fig. 5. Characterization of anti-SC2 and anti-SC2P3 antibodies in sera from SC2- or SC2P3-immunized rats using affinity chromatography. To characterize the nature of anti-SC2 and anti-SC2P3 antibodies in more detail, affinity columns coupled with either SC2P3 (A and B) or all the SC2 peptides (P1–P12) (C) were prepared and sera from SC2-immunized (A and C) or SC2P3-immunized (B) rats were passed through the columns. Then, the specificity of the eluate and flowthrough was analyzed by ELISA. When sera from SC2-immunized rats were applied to the SC2P3-coupled column, the eluate contained antibodies that reacted with SC2 and SC2P3 (Eluate A). In contrast, there were anti-SC2, but not anti-SC2P3, antibodies in the flowthrough fraction (Flow through A). Sera from SC2P3-immunized rats were also applied on the SC2P3-coupled column. In this case, all the anti-SC2 and anti-SC2P3 antibodies were captured on the column (Eluate B vs. Flow through B). Characteristically, sera from SC2-immunized rats contained antibodies that reacted with non-linear epitopes (Flow through C).

3.5 or 4 in each group. As clearly demonstrated in Fig. 4, SC2 induced inflammatory lesions with Scores 3–3.5 and 4 (Fig. 4A), whereas SC2P3 induced only mild lesions with Score 1–1.5 (Fig. 4B). Severe lesions with Score 2–2.5, 3–3.5, or 4 were not found in the latter group. Immunization with a higher dose of SC2P3 (300 μg) resulted in the formation of intermediately severe lesions with Score 2–2.5, but not of lesions with Score 3–3.5, or 4 (Fig. 4C). These findings strongly suggest that although SC2P3 contains major myositogenic epitope(s), it lacks factors that aggravate inflammatory lesions as found in SC2-induced EAM.

3.5. Characterization of autoantibodies generated after immunization with SC2 or SC2P3

The above findings raised the possibility that anti-SC2 antisera contain highly pathogenic antibodies that were absent in the SC2P3 antiserum preparation. To characterize the nature f the anti-SC2 antibodies in more detail, we prepared affinity columns coupled with either SC2P3 or all the SC2 peptides (P1–P12). Then, sera from SC2- or SC2P3-immunized rats were passed through the columns and the specificity of the eluate and flowthrough was analyzed by ELISA. The results are illustrated in Fig. 5. When sera from SC2-immunized rats were applied to the SC2P3-coupled column, the eluate contained antibodies that reacted with SC2 and SC2P3 (Eluate A of Fig. 5A). In contrast, there were anti-SC2, but not anti-SC2P3, antibodies in the flowthrough fraction (Flow through A of Fig. 5A). Similarly, sera from SC2P3-immunized rats were applied to the SC2P3-coupled column. In this case, all the anti-SC2 and anti-SC2P3 antibodies were captured on the column (Eluate B vs. Flow through B in Fig. 5B). Furthermore, Flow through C of anti-SC2 antisera that had been passed through the SC2P1-12 column contained anti-SC2 antibodies (Fig. 5C). These findings imply that anti-SC2 antisera contain anti-SC2 antibodies, possibly against the conformational epitope of the SC2 molecule, that do not bind with any of the SC2 peptides. In contrast, anti-SC2P3 antisera contained antibodies only reacting with SC2P3 (see Flow through B of Fig. 5B).

Table 5
SC2 peptide immunization plus antibody transfer experiments in EAM[a]

Group	Immunization	Ab transfer		Inflammation	
		Ab	Dose	Incidence	Score
A	SC2P5	Anti-SC2 sera	×5 dil (1 ml) × 2/w×3	3/3	0.28±0.09
B	SC2P5	SC2P mAb mix	2 mg×2/w×3	3/3	0.28±0.11
C	SC2P5	SC2P3.1 mAb (IgG1)	1 mg×2/w×3	3/3	0.28±0.11
D	SC2P5	SC2.1 mAb (IgG1)	1 mg×2/w×3	3/3	0.22±0.10
E	SC2P3	SC2.16 mAb (IgG2a)	1 mg×2/w×3	3/3	0.92±0.46
F	SC2P3	Saline	×2/w×3	3/3	0.67±0.46

[a] SC2P5 or SC2P3 peptide was immunized and the indicated sera (1 ml after 5-fold dilution) or mAb were injected intravenously twice a week for 3 weeks. Rats were examined histologically 2 weeks after the last antibody administration.

3.6. SC2 peptide immunization with co-transfer of anti-SC2 antibodies

Finally, we have tried to reproduce severe EAM compatible with SC2-induced EAM by SC2 peptide immunization plus co-transfer of polyclonal or monoclonal anti-SC2 antibodies (Table 5). Immunization with SC2P5 that contains the T cell epitope plus transfer of various types of anti-SC2 antibodies did not augment the severity of EAM (Groups A–D) compared with SC2P5 immunization alone (Table 4, Group F). SC2P3 immunization plus antibody transfer induced more severe EAM than SC2P3 immunization plus saline but there was no significant difference between the two groups (Group E vs. Group F). Thus, co-administration of anti-SC2 antibodies resulted in slight aggravation of peptide-induced AM but could not reproduce SC2-induced EAM.

4. Discussion

Polymyositis and dermatomyositis are muscle diseases characterized by the presence of muscle weakness and inflammatory infiltrates in the skeletal muscles (Dalakas, 1991). Although autoimmune processes are thought to be involved in the disease progression, these processes remain poorly understood. This is partly because there has been no good animal model for the detailed analysis. In a previous study (Kohyama and Matsumoto, 1999), we found that purified C-protein, a myosin-binding protein that comprises only 2% of the muscle components, possesses strong myositogenicity comparable with crude myosin and that its activity is much stronger than that of purified myosin. However, purified native C-protein has several limitations for detailed analysis. C-protein is a minor component of muscle proteins and therefore it is difficult to obtain a large amount of the protein (Offer, 1972; Offer et al., 1973). In addition, the purity and myositogenicity of the protein varied greatly from lot to lot, resulting in variation in the induction of EAM. In the present study, we characterized the role of pathogenic T and B cells in EAM hat had been induced by immunization with recombinant skeletal C-protein. Consequently, we obtained the following findings. First, all of the four recombinant C-protein fragments possessed myositis-inducing ability, indicating that the C-protein molecule contains multiple myositogenic epitopes. Second, in Fragment 2 of skeletal C-protein (SC2), which constantly induced severe EAM in Lewis rats, major T and B cell epitopes reside in SC2P5 (residues 84–412) and SC2P3 (residues 334–363), respectively. However, immunization with SC2P3, induced EAM but SC2P5 did not. Such discrepancy between the T and B cell epitopes was already observed in another autoimmune disease model. In experimental autoimmune encephalomyelitis (EAE) induced in Lewis rats by immunization with myelin basic protein MBP), the immunodominant epitope for encephalitogenic T cells resides within the 68–88 residues throughout the course of EAE (Vandenbark et al., 1985). In contrast, anti-MBP antibodies in the same strain react mainly with the 11–30 and 91–110 residues (Figueiredo et al., 1999).

It has been frequently reported that both autoreactive T cells and autoantibodies are involved in the pathogenesis of human PM. Clonal expansions of T cells, especially those bearing the CD8 phenotype, were observed in the peripheral blood of PM patients (Nishio et al., 2001; van der Meulen et al., 2002) and $CD8^+$ T cells with a similar characteristic infiltrated the muscle lesions (Arahata and Engel, 1984). In the present experiments, we demonstrated that T cells from SC2-immunized rats reacted only with SC2P5 but that SC2P5 immunization did not elicit EAM. These results suggest that simultaneous activation of pathogenic T and B cells is essential for the development of full-blown EAM.

With regard to autoantibodies in PM, there have been a number of reports demonstrating the presence of myositis-specific autoantibodies (MSA) (Brouwer et al., 2001; Mimori, 1999). For instance, anti-Jo-1 antibodies that recognize histidyl-tRNA synthetase are found in 20–30% of PM/DM patients. However, the role of MSA in the pathogenesis of PM remains almost unknown. Walker and Jeffrey speculated that through molecular mimicry among virus particles, Jo-1 antigen and muscle components such as myosin, autoantibodies raised after viral infection may attack Jo-1 antigen and the muscle (Walker and Jeffrey, 1986). Although it is possible, there is no direct evidence supporting this hypothesis. Curiously, there are no reports examining the presence or absence of autoantibodies against muscle components. As shown in the present study, autoantibodies against muscle components such as C-protein play a critical role in the development and progression of inflammatory myopathies. In sharp contrast to this situation, it was already demonstrated that anti-myocardial autoantibodies are present in patients with myocarditis and dilated cardiomyopathy (DCM) (Baba et al., 2001; Caforio et al., 2001, 2002) and removal of such antibodies by immunoadsorption induced early hemodynamic improvement (Felix et al., 2002).

On the basis of the findings obtained in T cell and autoantibody analysis, we tried to induce EAM comparable with SC2-induced EAM by SC2 peptide immunization plus adoptive transfer of various types of anti-SC2 antibodies, either polyclonal or monoclonal. Although co-transfer of anti-SC2 antibodies augmented the severity of SC2 peptide-induced EAM, we failed to induce full-blown EAM by this procedure. Furthermore, we have tried to induce passive EAM by adoptive transfer of SC2- or SC2 peptide-reactive T cells but failed to induce the disease. At least, two possibilities should be considered. First, it is possible that our protocol for antibody administration did not maintain sufficient antibody levels for lesion formation. The second possibility is that the barrier at the interface between the blood vessels and skeletal muscle (Dow et al., 1980) is so tight that the antibodies cannot enter muscle fibers even with the help of activated T cells. In this regard, it is interesting to note the results obtained in experimental autoimmune carditis (EAC). We already reported that EAC is inducible by immunization with cardiac C-protein fragment 2 (CC2) (Matsumoto et al., 2004) and observed B cell epitope spreading in rats that had been immunized with CC2, but not with CC2 peptide. In this case, peptide immunization plus anti-CC2 antibodies aggravated EAC (Matsumoto et al., 2007). Of course, these two possibilities do not exclude each other.

In summary, we have successfully induced EAM by immunization of recombinant SC2, and determined the myositogenic sequence in the SC2 molecule and the T and B cell epitopes. The data obtained in the present study provide useful information to analyze the pathomechanisms of the disease and to develop specific immunotherapies for PM in the near future.

Acknowledgements

This study was supported in part by Health and Labour Sciences Research Grants for Research on Psychiatric and Neurological Diseases and Mental Health and by Grants-in-Aid from the Japan Society for the Promotion of Science.

References

Arahata, K., Engel, A.G., 1984. Monoclonal antibody analysis of mononuclear cells in myopathies. I: Quantitation of subsets according to diagnosis and sites of accumulation and demonstration and counts of muscle fibers invaded by T cells. Ann. Neurol. 16, 193–208.

Baba, A., Yoshikawa, T., Chino, M., Murayama, A., Mitani, K., Nakagawa, S., Fujii, I., Shimada, M., Akaishi, M., Iwanaga, S., Asakura, Y., Fukuda, K., Mitamura, H., Ogawa, S., 2001. Characterization of anti-myocardial autoantibodies in Japanese patients with dilated cardiomyopathy. Jpn. Circ. J 65, 867–873.

Brouwer, R., Hengstman, G.J., Vree Egberts, W., Ehrfeld, H., Bozic, B., Ghirardello, A., Grondal, G., Hietarinta, M., Isenberg, D., Kalden, J.R., Lundberg, I., Moutsopoulos, H., Roux-Lombard, P., Vencovsky, J., Wikman, A., Seelig, H.P., van Engelen, B.G., van Venrooij, W.J., 2001. Autoantibody profiles in the sera of European patients with myositis. Ann. Rheum. Dis. 60, 116–123.

Caforio, A.L., Mahon, N.J., McKenna, W.J., 2001. Cardiac autoantibodies to myosin and other heart-specific autoantigens in myocarditis and dilated cardiomyopathy. Autoimmunity 34, 199–204.

Caforio, A.L., Mahon, N.J., Tona, F., McKenna, W.J., 2002. Circulating cardiac autoantibodies in dilated cardiomyopathy and myocarditis: pathogenetic and clinical significance. Eur. J. Heart Fail. 4, 411–417.

Dalakas, M.C., 1991. Polymyositis, dermatomyositis, and inclusion-body myositis. New Engl. J. Med. 325, 1487–1498.

Dalakas, M.C., 1992. Inflammatory Myopathy. Handbook of Clinical Neurology, Vol. 18(61). Elsevier, Amsterdam, pp. 369–390.

Dennis, J.E., Shimizu, T., Reinach, F.C., Fischman, D.A., 1984. Localization of C-protein isoforms in chicken skeletal muscle: ultrastructural detection using monoclonal antibodies. J. Cell Biol. 98, 1514–1522.

Dow, P.R., Shinn, S.L., Ovale Jr., W.K., 1980. Ultrastructural study of a blood-muscle spindle barrier after systemic administration of horseradish peroxidase. Am. J. Anat. 157, 375–388.

Engel, A.G., Arahata, K., 1984. Monoclonal antibody analysis of mononuclear cells in myopathies. II: Phenotypes of autoinvasive cells in polymyositis and inclusion body myositis. Ann. Neurol. 16, 209–215.

Felix, S.B., Staudt, A., Landsberger, M., Grosse, Y., Stangl, V., Spielhagen, T., Wallukat, G., Wernecke, K.D., Baumann, G., Stangl, K., 2002. Removal of cardiodepressant antibodies in dilated cardiomyopathy by immunoadsorption. J. Am. Coll. Cardiol. 39, 646–652.

Figueiredo, A.C., Cohen, I.R., Mor, F., 1999. Diversity of the B cell repertoire to myelin basic protein in rat strains susceptible and resistant to EAE. J. Autoimmun. 12, 13–25.

Fischman, D.A., Vaughan, K., Weber, F., Einheber, S., 1991. Myosin Binding Proteins: Intracellular Members of the Immunoglobulin Superfamily. Frontiers in muscle research, pp. 211–222.

Jefferies, W.A., Green, J.R., Williams, A.F., 1985. Authentic T helper CD4 (W3/25) antigen on rat peritoneal macrophages. J. Exp. Med. 162, 117–127.

Kohyama, K., Matsumoto, Y., 1999. C-protein in the skeletal muscle induces severe autoimmune polymyositis in Lewis rats. J. Neuroimmunol. 98, 130–135.

BRAIN RESEARCH 1162 (2007) 113–120

available at www.sciencedirect.com

ScienceDirect

www.elsevier.com/locate/brainres

BRAIN RESEARCH

Research Report

Increased phosphorylation of cyclic AMP response element-binding protein in the spinal cord of Lewis rats with experimental autoimmune encephalomyelitis

Heechul Kim[a,1], *Changjong Moon*[b,1], *Meejung Ahn*[a], *Yongduk Lee*[a], *Seungjoon Kim*[a], *Yoh Matsumoto*[c], *Chang-Sung Koh*[d], *Moon-Doo Kim*[e], *Taekyun Shin*[a,*]

[a]*Department of Veterinary Medicine and Applied Radiological Science Research Institute, Cheju National University, Jeju 690-756, South Korea*
[b]*Department of Veterinary Anatomy, College of Veterinary Medicine, Chonnam National University, Gwangju 500-757, South Korea*
[c]*Department of Molecular Neuropathology, Tokyo Metropolitan Institute for Neuroscience, Fuchu, Tokyo 183, Japan*
[d]*Department of Biomedical Laboratory Sciences, Shinshu University School of Health Sciences, 3-1-1 Asahi, Matsumoto 390-8621, Japan*
[e]*Department of Psychiatry, Cheju National University College of Medicine, Jeju 690-756, South Korea*

ARTICLE INFO

Article history:
Accepted 31 May 2007
Available online 21 June 2007

Keywords:
Astrocyte
Cyclic AMP response element-binding protein (CREB)
Experimental autoimmune encephalomyelitis (EAE)
Macrophage
Neuron

ABSTRACT

To investigate whether the phosphorylation of cyclic AMP response element-binding protein (CREB) is implicated in the pathogenesis of experimental autoimmune encephalomyelitis (EAE), the change in the level of CREB phosphorylation was analyzed in the spinal cord of Lewis rats with EAE. Western blot analysis showed that the phosphorylation of CREB in the spinal cord of rats increased significantly at the peak stage of EAE compared with the controls ($p<0.05$) and declined significantly in the recovery stage ($p<0.05$). Immunohistochemistry showed that the phosphorylated form of CREB (p-CREB) was constitutively immunostained in few astrocytes and dorsal horn neurons in the spinal cord of normal rats. In the EAE-affected spinal cord, p-CREB was mainly found in ED1-positive macrophages at the peak stage of EAE, and the number of p-CREB-immunopositive astrocytes was markedly increased in the spinal cord with EAE compared with the controls. Moreover, p-CREB immunoreactivity of sensory neurons, which are closely associated with neuropathic pain, was significantly increased in the dorsal horns at the peak stage of EAE. Based on these results, we suggest that the increased phosphorylation of CREB in EAE lesions was mainly attributable to the infiltration of inflammatory cells and astrogliosis, possibly activating gene transcription, and that its increase in the sensory neurons in the dorsal horns is involved in the generation of neuropathic pain in the rat EAE model.

* *Corresponding author*. Fax: +82 64 756 3354.
E-mail address: shint@cheju.ac.kr (T. Shin).
[1] The first two authors contributed to this work equally.

0006-8993/$ – see front matter © 2007 Elsevier B.V. All rights reserved.
doi:10.1016/j.brainres.2007.05.072